Investigating Past and Present Carpometacarpus Morphology in Mimidae: A Multi-Methods Approach to Evidence from the Guadeloupe Islands

Nicolas Jeantet, Ronan Ledevin, Monica Gala, Arnaud Lenoble, Frédéric Santos, Véronique Laroulandie

OPENQUATERNARY

Investigating Past and Present Carpometacarpus Morphology in Mimidae: A Multi-Methods Approach to Evidence from the Guadeloupe Islands

RESEARCH PAPER

NICOLAS JEANTET
RONAN LEDEVIN
MONICA GALA
ARNAUD LENOBLE
FRÉDÉRIC SANTOS
VÉRONIQUE LAROULANDIE

*Author affiliations can be found in the back matter of this article

]u[ubiquity press

ABSTRACT

Past bird communities are still under-studied in several Caribbean regions, including the Lesser Antilles. In order to improve our understanding of this area's avifauna, we explore morphometrical variations of the carpometacarpus (CMC) within West Indies Mimidae species. We combine geometric morphometric (GMM) and conventional osteology focusing on characters of the entire or distal portion of the CMC. Morphological variation related to their phylogenetic history is investigated using uni- and multi-variate statistics, and the expression of certain osteological characters. Fossil bone remains from the Guadeloupe Islands were included in the datasets to test the applicability of these results to the archaeological and paleontological record.

Our results are consistent with the known phylogeny of Mimidae. The GMM analysis clearly differentiated taxa at both inter- and intra-generic levels, which when combined with osteological characters, allow fossil specimens to be determined to species. For the fossil record of Guadeloupe Islands, this concerns three taxa: the Scaly-breasted Thrasher *Allenia fusca*, the Gray Catbird *Dumetella carolinensis*, the first fossil occurrence of this bird in the Greater and Lesser Antilles, and the Brown Trembler *Cinclocerthia ruficauda* in Desirade and Marie-Galante, where the bird is now extirpated. These results are of particular interest for tracking the impact of environmental changes on the composition of West Indian bird communities.

CORRESPONDING AUTHOR:
Arnaud Lenoble
PACEA UMR 5199, Université de Bordeaux, CNRS, MCC, France
arnaud.lenoble@u-bordeaux.fr

KEYWORDS:
Passeriformes; Lesser Antilles; past avian communities; geometric morphometric; osteology

TO CITE THIS ARTICLE:
Jeantet, N, Ledevin, R, Gala, M, Lenoble, A, Santos, F and Laroulandie, V. 2021. Investigating Past and Present Carpometacarpus Morphology in Mimidae: A Multi-Methods Approach to Evidence from the Guadeloupe Islands. *Open Quaternary,* 7: 10, pp. 1–27. DOI: *https://doi.org/10.5334/oq.99*

INTRODUCTION

The analysis of fossil bird bones from the West Indies has provided a wealth of information concerning the region's past avian communities (e.g., Olson & Hilgartner 1982; Pregill, Steadman & Watters 1994; Steadman & Franklin 2020). While it is now clear that many changes in this region's avifauna, including the disappearance of endemic species, followed the arrival of humans during the Holocene (e.g., Steadman, Pregill & Olson 1984; Steadman & Takano 2013), important data at a larger regional scale is still lacking (Orihuela et al. 2020; Steadman & Franklin 2020). The species-level identification of bird bones from archaeological and paleontological sites is therefore crucial for exploring past bird communities, especially as it potentially allows a chronology to be built for the earliest and latest occurrences of particular taxa. Although researchers typically rely on comparative osteological collections to identify specimens, such an approach has important limitations in the Caribbean. The region's avian communities are highly diverse due to high island endemism that is poorly reflected in current avian osteological collections (Lefevbre & Sharpe 2018; Steadman & Franklin 2017). Therefore, certain groups, such as passerine birds, and several sub-regions, including the Lesser Antilles, are still remarkably under-documented (Olson 1978). This lack of data hinders the identification of fossil bird remains and, as a consequence, our understanding of larger-scale diachronic changes in West Indian bird communities.

One bird family, Mimidae, is of particular interest for better exploring these issues. This New World family of passerine birds and their colonization of the Caribbean Islands is one of the best-known examples of avian radiation in the West Indies (Hunt, Bermingham & Ricklefs 2001; Ricklefs & Bermingham 2008). In this region, this family comprises five regional endemic species to which can be added five pan-continental species that differ in habit preference (dry vs. wet forest, closed vs. open environments) or stratum exploited (canopy vs. ground). The origin and phylogeny of this family is also well established, with their dispersal from North America currently being the most widely accepted hypothesis (Arbogast et al. 2006; Bond 1948, 1963; Lovette et al. 2012). In addition, molecular phylogeny shows modern specimens to occupy two main clades based on distribution: an endemic Antillean clade and a pan-continental clade (***Figure 1***; Cibois &

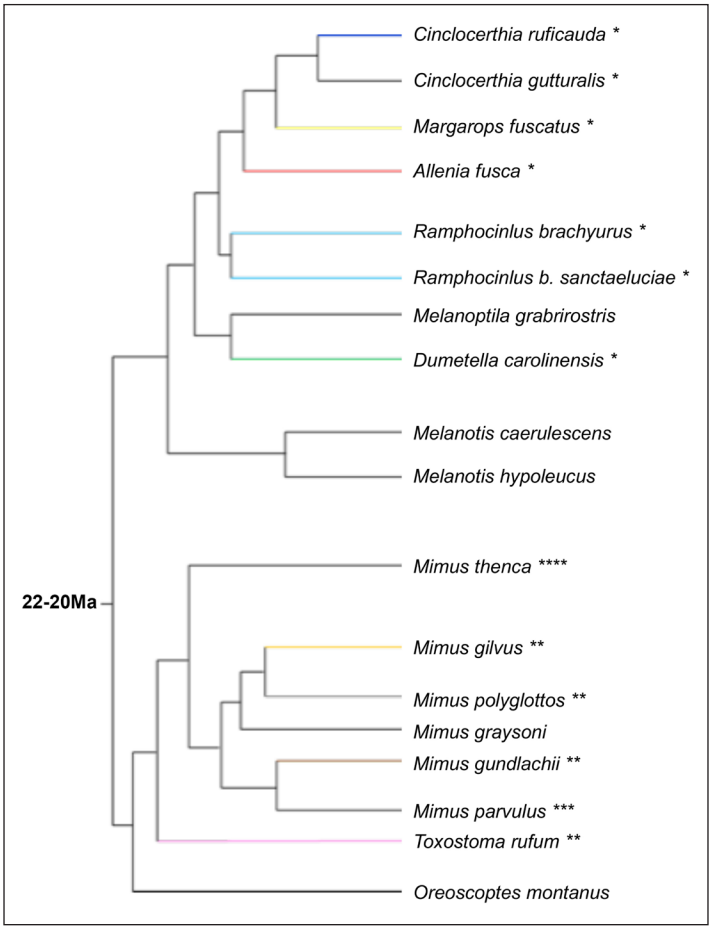

Figure 1 A simplified consensus phylogenetic tree for Mimidae based on mitochondrial and nuclear DNA (modified after Lovette et al. 2012: figure 1). The position of *Dumetella carolinensis* follows (DaCosta et al. 2019: figure 4). The colored branches represent taxa included in the study. * Species belonging to the Antillean endemic clade. ** Species belonging to the Pan-continental clade. *** Species endemic to the Galapagos Islands. **** Species endemic to South America.

Cracraft 2004; Hunt, Bermingham & Ricklefs 2001; Lovette & Rubenstein 2007). In this study, *Dumetella carolinensis* has been included within the West Indian endemics clade as previously suggested by Lovette and collaborators (2012). More recently, DaCosta et al. (2019) placed this passerine in a sister clade comprising all the West Indian species.

Here we investigate morphometric variation in a specific wing bone, the carpometacarpus (CMC), of Mimidae from the West Indies. While quantitative and qualitative osteological descriptions of the postcranial skeleton of European Passeriformes are available (e.g. Kessler 2015; Moreno 1985, 1986 and 1987; Tomek & Bochenski 2000; Wojcik 2002), none exist for the CMC of Mimidae, except for *Mimus gundlachii* (Tellkamp 2005). We focus on the CMC as it is a key element involved in flight and therefore has high potential as a taxonomic indicator (Mayr 2016). Furthermore, the CMC is relatively frequent in the archaeological and paleontological record (Bovy 2002). Moreover, the skeleton flight apparatus of Passeriformes has been shown to be "an interesting area to partition the relative contributions of adaptive correlated evolution and phylogenetic constraint to species clustering in morphological space" (Corbin, Lowenberger & Dorkoski 2013: 1).

We use classic osteological descriptions with geometric morphometrics (GMM) applied to 3D surface models of Mimidae CMC to investigate inter- and intra-generic phenotypic differences connected to the evolutionary history of this family and identify diagnostic characters of different present-day West Indian Mimidae species. These characters are then used to identify Mimidae fossil remains from the Guadeloupe Islands in order to generate a picture of this region's past avian community.

MATERIAL AND METHODS

MODERN SPECIMENS

The modern Mimidae sample comprises 55 specimens from 7 of the 10 genera of this family and 9 of 34 species known worldwide. The material comes from eight institutions and different geographic areas (see ***Table 1*** for

COMMON NAME	BINOMIAL NOMENCLATURE	CLADE	N	SIDE	OWNING INSTITUTION	ORIGIN	SEX
Grey Catbird	*Dumetella carolinensis*	Antillean endemics	5	L (2); R(3)	AMNH (1); NHM (3); USNM (2)	Florida (2); New Jersey (1); Kansas (1); indet (1)	F (4); indet (1)
White-breasted Thrasher	*Ramphocinclus brachyurus*		3	L (2); R(1)	MNHN (2); UMMZ (1)	Saint Lucia (2); Martinique (1)	F (1); indet (2)
Brown Trembler	*Cinclocerthia ruficauda*		5	L (2); R(3)	MEC (1); PACEA (4)	Guadeloupe islands (5)	F (1); M (1); indet (3)
Scaly-breasted Thrasher	*Allenia fusca*		16	L (9); R(7)	MEC (1); PACEA (15)	Guadeloupe islands (16)	F (1); M (3); indet (12)
Pearly-eyd Thrasher	*Margarops fuscatus*		8	L (4); R(4)	PACEA (8)	Guadeloupe islands (8)	F (1); M (4); indet (3)
Bahama Mockingbird	*Mimus gundlachii*	Pan-continental	5	L (2); R(3)	ROM (1); USNM (4)	The Bahamas (5)	F (3); M (2)
Tropical Mockingbird	*Mimus gilvus*		4	L (2); R(2)	MEC (1); PACEA (4)	Guadeloupe islands (3); indet (1)	F (1); indet (3)
Northern Mockingbird	*Mimus polyglottos*		6	L (2); R(4)	MNHN (2); NHM (1); ROM (1); USNM (2)	Florida (1); New Jersey (1); California (1); Mexico (1); Dominican Republic (1)	F (2); M (3); indet (1)
Brown Trembler	*Toxostoma rufum*		3	L (2); R(1)	MNHN (1), USNM (1); NHM (1)	Kansas (1), New York (1), Maryland (1)	M (3)

Table 1 Modern comparative sample used in this study. (**AMNH**) American Museum of Natural History, New York; (**MEC**) Edgar Clerc Museum, Le Moule; (**MNHN**) French National Museum of Natural History, Paris; (**NHMUK**) Natural History Museum, London; **(PACEA)** Laboratory of the University of Bordeaux; (**UMMZ**) University of Michigan Museum of Zoology, Ann Arbor; (**USNM**) National Museum of Natural History, Smithsonian Institution, Washington; (**ROM**) Royal Ontario Museum, Toronto. (**L**) = left, (**R**) = right, (**F**) = female, (**M**) = male, n = sample size.

more detail). All selected individuals are fully ossified and can be considered adult specimens. Sex data is available for only part of sample (see Supplementary file 1).

Ten members of the Mimidae family currently occur in the Caribbean, either as breeding or migrating populations (Raffaele et al. 2010), all of which were included in the analyzed sample, apart from the Grey Trembler *Cinclocerthia gutturalis*. As Caribbean vertebrate diversity is poorly represented in museum collections (Lefebvre & Sharpe 2018), the dataset required loans and the 3D modeling of specimens from various institutions (***Table 1***). In addition, the osteology of several rare and endangered species, such as the White-throated Thrasher *Ramphocinclus brachyurus* (Mortensen et al. 2017; Birdlife 2020), are represented by such a small number of specimens worldwide that sample construction equally required microscanning skin specimens.

FOSSIL SPECIMENS

Guadeloupe comprises two main islands, separated by a narrow stretch of sea. The slopes of the mountainous island of Basse-Terre, to the west, support a tropical rain forest (Supplementary file 2), connecting it to the group of wet islands forming the internal volcanic arc of the Lesser Antilles. The low and flat island of Grande Terre, in the east, is covered with dry deciduous or scrub forest, similar to the other dry limestone islands of the outer arc. The smaller islands of La Désirade, 15 km to the east, and Marie-Galante, 25 km to the south, also correspond to two limestone platforms of the outer arc. These limestone islands are favourable to the development of caves likely to preserve fossil deposits (Lenoble et al. 2009). These deposits produced several medium-sized Passeriformes, which based on comparisons with the PACEA laboratory (de la Préhistoire à l'Actuel: Culture, Environnement et Anthropologie) osteological bird collection (Lenoble, Gala & Laroulandie 2019) can be assigned to a Caribbean family of this order (e.g. Turdidae, Thraupidae, Icteridae, Mimidae). Mimidae bones have been recovered from excavations of several sites in the Guadeloupe islands: *Grotte Cadet 2*, *Abri Cadet 3* and *Grotte Blanchard* on Marie-Galante, *Grotte des Bambous* on Grande Terre, and *Pointe Gros Rempart 6* (PGR6) on La Désirade (***Table 2*** and Supplementary file 2). Here we refer to these bones as "fossil" in order to distinguish them from the modern specimens. The bones were recovered from natural deposits, some of which either predate (*Grotte Blanchard*, *Grotte Cadet 2*) or are contemporaneous with the presence of humans on the islands (*Abri Cadet 3*, *Pointe Gros Rempart*, *Grotte des Bambous*). While the occasional human occupation of the latter sites can not be excluded, the formation of the deposits and accumulation of bones is primarily non-anthropogenic (Boudadi-Maligne et al. 2016; Cochard et al. 2019). These collections have been built over the past decade as part of the Bivaag (« *Biodiversité insulaire vertébrée ancienne des îles de Guadeloupe* ») and ECSIT (« *Écosystèmes insulaires tropicaux, réponse de la faune indigène terrestre de Guadeloupe à 6 000 ans d'anthropisation du milieu* ») research projects carried out at the PACEA laboratory, both focusing on the past biodiversity and ecology of Guadeloupe. We selected twelve CMC from these collections (***Table 2***) for 3D modeling and comparison with the modern specimens. All bones come from adult individuals and present various states of preservation (whole, sub-complete).

LOCATION	SPECIMEN LABEL	SITE	CONTEXT	LAYER	CHRONOLOGY	REFERENCES
Grande-Terre, Guadeloupe	BAM-2014-O-20	*Grotte des Bambous*	surface	–	0.7 ka BCE – 1.9 ka CE	Cochard et al. 2019
Marie-Galante	AC3-2019-O-1435	*Abri Cadet 3*	F3c – split 19	layer 3	3 ka BCE – 1 ka CE	Stouvenot et al. 2014
	GB-2008-O-349	*Grotte Blanchard*	Test-pit H33 – split 20	layer 5	11.3 ka BCE	Gala & Lenoble 2015; Stoetzel et al. 2016; Royer et al. 2017
	GB-2008-O-361		Test-pit H33 – split 18	layer 5		
	GB-2014-O-35		I33a – split 29	layer 5		
	GB-2014-O-92		I33d – split 30	layer 5		
	GB-2014-O-156		H33d – split 21	layer 10	27.9 ka BCE	
	GC2-2014-O-1	*Grotte Cadet 2*	026 – split 1	U4'	0.5 CE – 11.5 ka BCE	Lenoble 2014; Bochaton et al. 2015
	GC2-2014-O-2		O26 – split 3	U5a	11.5 -14.4 ka BCE	
La Désirade	PGR6-2011-O-16	*Pointe Gros Rempart 6*	Test-pit – split 4	layer 1/2	–	Boudadi-Maligne et al. 2016
	PGR6-2011-O-51		Test-pit – split 5	layer 2	1.7 – 1.95 CE	
	PGR6-2016-O-182		C11c – split 18	layer 3	0 – 1.7 ka CE	

Table 2 Fossils sample for the study. The chronology for *Grotte Blanchard* is the average age model proposed by Royer et al. (2017). BCE: Before Common Era; CE: Common Era.

OSTEOLOGICAL CHARACTERS AND METRICS

Osteological terminology follows Baumel and Witmer (1993) and Tomek and Bochenski (2000). Frequencies of character state were established on both 3D scans and the osteological material. The scoring was repeated two or three times by four of the co-authors (NJ, MG, VL, AL) in order to ensure the robustness of the consensus definition of characters and reproducibility of the coding. A threshold of an 80% frequency of character states was fixed in order to separate diagnostic and non-diagnostic characters. This choice allows possible outliers to be retained while at the same time preserving a high frequency value considering the limited number of specimens of most of the taxa in the study.

Greatest length (GL) measurements were recorded following Von Den Driesch (1976) and those of the breadth of the distal end (Bd) of the CMC following Kessler (2015). Measurements were taken using the Avizo software package for 3D scans or with a digital caliper.

MICRO-CT AND 3D IMAGING

All but one of the CMC were scanned with General Electric Vtome x|s x-ray microtomograph of the PACEA laboratory (housed at the UMS Placamat, University of Bordeaux, France) using a source voltage of 100 kV, 120 µA source current, 500 ms exposure time, 2550 projections, and 0.1 mm copper filter. Voxel sizes of the acquisitions ranged between 10 and 17 microns, depending on the specimen. For conservation reasons, one of the White-Breasted Thrasher CMC (UMMZ-158596) was scanned at the host institution. Surface models were generated with the Avizo *Isosurface* module (version 9.3.0) using all voxels with a greyscale value above a selected threshold (Wils 2016). This type of surface model provides more detail than volume rendering techniques (Weber & Bookstein 2011) and generates triangulated surfaces that can be easily manipulated and measured. When CMC were still connected to adjacent bones, a "semi-automatic" segmentation of the CMC was performed in order to isolate the area of interest and generate a corresponding 3D surface model.

GEOMETRIC MORPHOMETRIC ANALYSIS

Only left CMC were retained for analysis or, if the left bone was broken, a mirror image of the complete right CMC was substituted. Centroid size, which corresponds to the square root of the sum of the squares of the distances between its center of gravity and each of its points (Bookstein 1997), was used as a proxy for body size. Shape variation was analyzed using 256 semi-landmarks and 5 landmarks on the modeled surfaces. These points were placed along 15 curves of interest using Avizo (version 9.3.0; Supplementary file 3). Semi-landmarks were slid along a tangent to the curve using the minimum bending energy criterion to minimize differences in conformation between structures (Cucchi et al. 2015; Mitteroecker & Gunz 2009; Weber & Bookstein 201). These points were then projected onto the analyzed surface. A three-step procrustes superimposition (translation, normalization, and rotation of the original landmark data) was performed to compare the geometric conformations of the analyzed specimens (Cucchi et al. 2015; Mitteroecker & Gunz, 2009). All analyses were performed using R3.5.3 (R Core Team, 2019).

Four well-preserved and complete fossil CMC were compared to those from modern Mimidae. In order to include more specimens in the analysis, the number of landmarks was reduced for several poorly-preserved CMC where the targeted shape curves were compromised. The 31 landmarks positioned on the distal part of bones allowed eight specimens to be added, for an overall sample of 12 fossil specimens. The distal portion of the 12 specimens was then reanalyzed as a whole. A similar approach was applied to the proximal portion of the CMC, which produced less reliable discrimination of taxa. We therefore chose to present only the results for the distal portion of the CMC.

STATISTICAL ANALYSIS

CMC centroid size differences were explored within and between groups using analyses of variance (ANOVA). In order to investigate inter-specific and inter-generic shape variation, we performed a principal component analysis (PCA) of the procrustes coordinates. In order to identify overlap between genera or species, convex hulls were generated in the different morphospaces. As the number of specimens is limited in our sample, we performed MANOVAs on the most significant axes of the PCA in order to limit the number of input variables. A preliminary threshold was defined and only axes explaining at least 5% of the total variance were considered when testing for potential differences between groups. We then created a dendrogram to visualize shape proximities between taxa based on multiple axes. Finally, a linear discriminant analyses using the same PC scores as input variables were performed to predict genera and species as well as to calculate the proportion of specimens attributed to each Mimidae genus and species.

Fossil specimens were inserted as additional individuals in the initial PCA but were excluded from the calculation of the principal component axes. A hierarchical clustering was then performed on the first five axes of the PCA. All statistics and visualizations were produced using R 3.5.3 (R Core Team, 2019) and the R packages *Morpho* (Schlager 2017), *ade4* (Dray & Dufour 2007), *rgl* (Adler & Murdoch 2019), and *geomorph* (Adams et al. 2019).

Confusion matrices based on a linear discriminant analysis were performed on the first five axes to reassign modern specimens to their original genus and then attempt the same with the fossil specimens. Results were considered statistically significant when p-values were less than 0.05.

RESULTS

OSTEOLOGICAL CHARACTERS AND METRICS

At the family level, Mimidae CMC are slenderer than those from Turdidae, with the shape of proximal portion of the *trochlea carpalis* differentiating them from other middle-sized passerine birds.

Five distinguishing characters (1 proximal and 4 distal; ***Figures 2*** and ***3***), each presenting two morphological states, were identified on complete CMC.

The first character (A) concerns a ridge in the proximal part of the *os metacarpale minus*, in dorsal view. In state 1 (A1 typical) this ridge joins the *facies articularis ulnocarpalis* to the *processus intermetacarpalis* and delimits cranially a facet developed on the caudal edge. In *Cinclocerthia*, this facet is sometimes very slight (PACEA-O-846) while the concavity of the cranial edge is highly pronounced and characteristic of this taxon. This ridge can be weakly developed distally while still clearly connected to the base of the *facies articularis ulnocarpalis* (A1 extrem). In state 2, this ridge is almost imperceptible or rapidly disappears, merging with the first half the intermetacarpal space above the intermetacarpal process or just beyond it (A2 typical). In all cases, the dorsal surface between the intermetacarpal space and the *trochlea* is uniformly flat. In *Mimus*, this facet can be broad, and the ridge is weakly developed in the distal portion and does not join the *trochlea carpalis* (A2 extrem).

The second character (B) concerns the inclination of the *facies articularis digitalis minor* in ventral view. In state 1, this facies is clearly inclined with the caudal edge which projects further distally than the cranial edge; the angle defined by the line between the two edge extremities and the proximo-distal axis is greater than 8° (B1 typical). The distal end of the bone curves dorsally, which reduces the angle (B1 extrem). However, the angle is greater than 8° when the distal extremity of the bone is positioned in front of the observer. In state 2, the caudal and cranial edges have a broadly comparable distal extension (B2 typical). B2 is extreme when the caudal edge extends more distally but the angle between the edge extremities and the proximo-distal axis remains lower than 8°.

The third character (C) concerns the morphology of the *facies articularis digitalis minor* in ventral view. In state 1 (C1 typical), a groove is present. This groove can be weakly developed, hardly distinguishable from an irregularity of the articular surface (C1 extrem). This groove is absent in state 2 (C2 typical) or not developed enough to be appreciable (C2 extrem).

The fourth character (D) is observable on the distal part of the *sulcus tendineus* in dorsal view. In state 1, the cranial and caudal ridges of the *sulcus tendineus* extend distally (D1 typical). The cranial ridge can extend less distally than the caudal ridge, with the angle between the ridge extremities and the cranio-caudal axis measuring

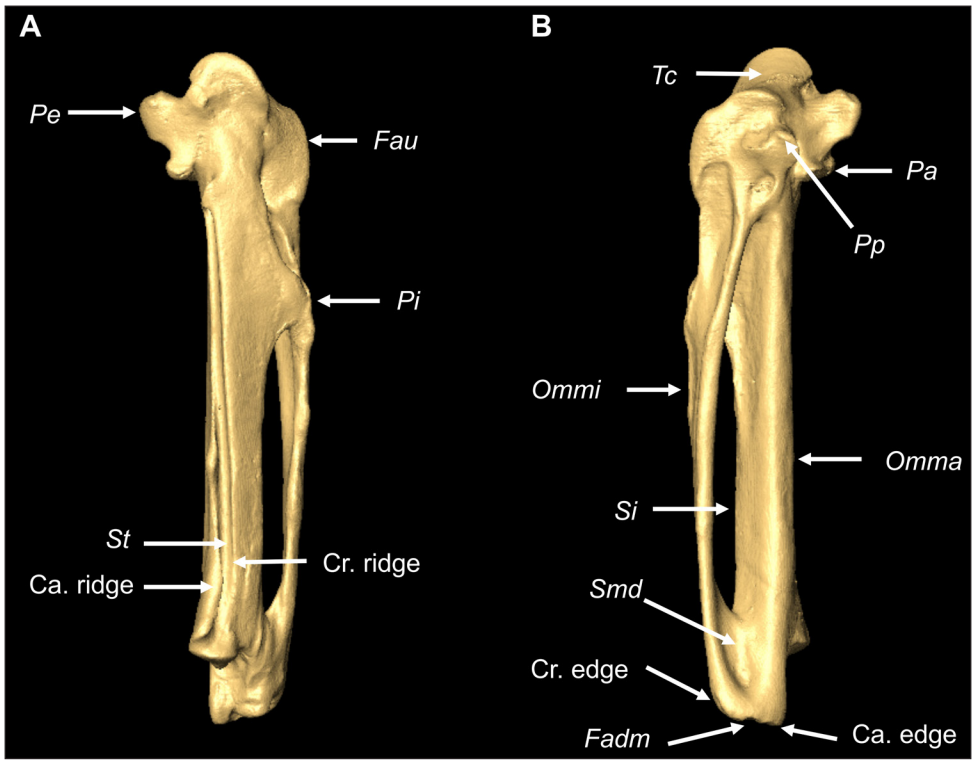

Figure 2 Terminology used for the osteological characters of the CMC. 3D model of a left CMC from *Mimus gundlachii* (ROM 111017) in dorsal **(A)** and ventral **(B)** views. Ca. edge: Caudal edge of the distal part; Ca. ridge: Caudal ridge; Cr. edge: Cranial edge of the distal part; Cr. ridge: Cranial ridge; Fadm: *Facies articularis digitalis minor*; Fau: *Facies articularis ulnocarpalis*; Omma: *Os metacarpale major*; Ommi: *Os metacarpale minus*; Pa: *Processus alularis*; Pe: *Processus extensorius*; Pi: *Processus intermetacarpalis*; Pp: *Processus pisiformis*; Si: Spatium intermetacarpalis; *Smd: Symphysis metacarpalis distalis*; St: *Sulcus tendineus*; Tc: *Trochlea carpalis*.

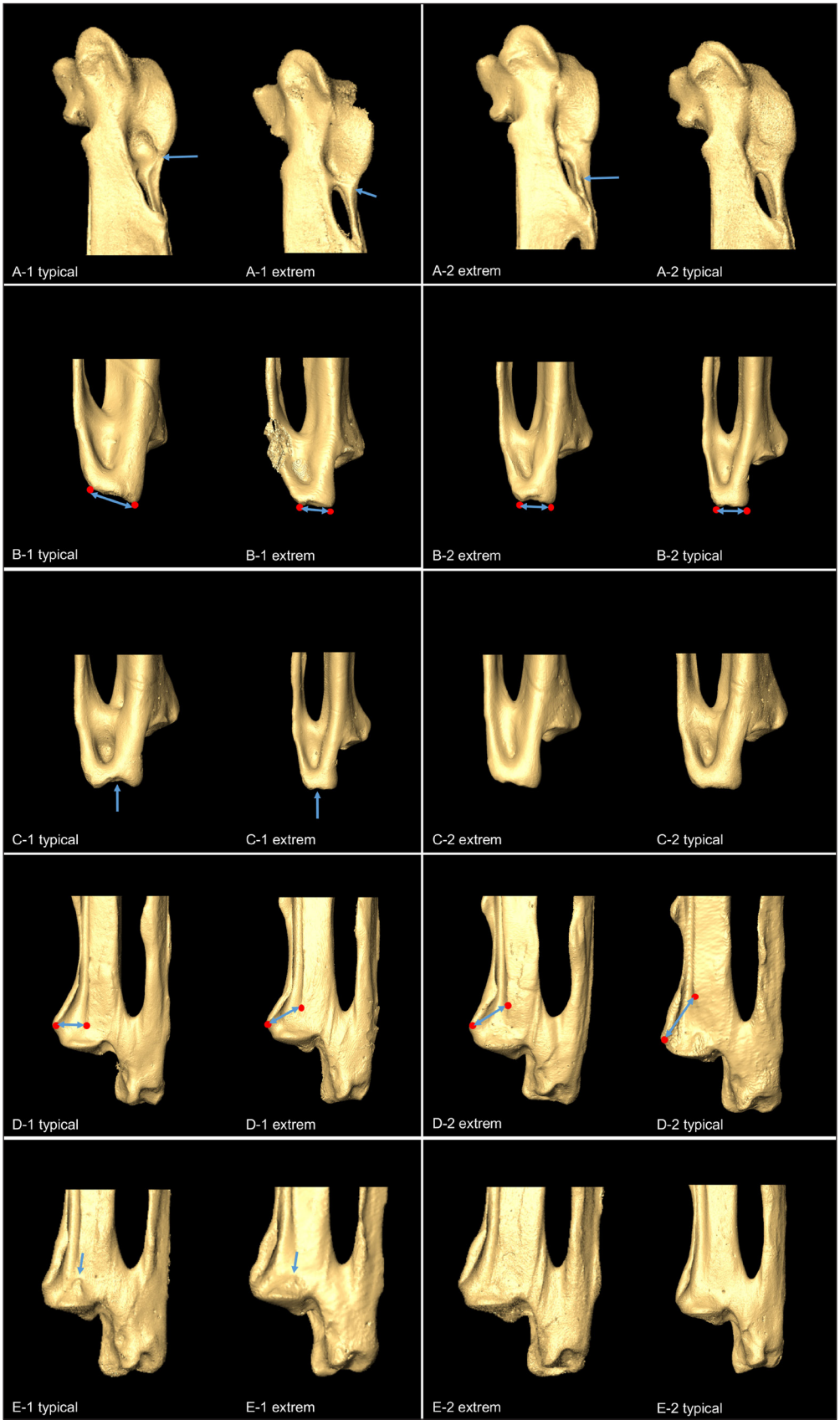

Figure 3 Identified character states. Blue arrows indicate zones of interest. Specimens used for the characters: **A-1 typical**: *Allenia fusca*, PACEA-O-1043; **A-1 extrem**: *Dumetella carolinensis*, NHMUK ZOO S/2010.2.15; **A2 typical**: *Mimus gilvus*, PACEA-O-733; **A2 extrem**: *Mimus gundlachii*, ROM 111017; **B-1 typical**: *Mimus gundlachii* USNM 553337; **B-1 extrem**: *Ramphocinclus brachyurus*, MNHN ZO 2012-550; **B-2 typical**: *Allenia fusca*, PACEA-O-1042; **B-2 extrem**: *Margarops fuscatus*, PACEA-O-1039; **C-1 typical**: *Margarops fuscatus*, PACEA-O-1041; **C-1 extrem**: *Allenia fusca*, PACEA-O-1042; **C-2 typical**: *Margarops fuscatus*, PACEA-O-731; **C-2 extrem**: *Mimus gundlachii*, ROM 111017; **D-1 typical**: *Allenia fusca*, PACEA-O-1042; **D-1 extrem**: *Allenia fusca*, PACEA-O-1048; **D-2 typical**: *Mimus polyglottos*, MNHN ZO MO-1933-306; **D-2 extrem**: *Toxostoma rufum*, USNM 611207 **E-1 typical**: *Mimus gundlachii*, USNM 553450; **E-1 extrem**: *Mimus polyglottos*, MNHN ZO MO-1956-1050; **E-2 typical**: *Mimus gilvus*, PACEA-O-732; **E-2 extrem**: *Cinclocerthia ruficauda*, PACEA-O-966.

less than 10° (D1 extrem). In state 2, the extremity of the cranial ridge is occupied by the *sulcus tendineus*, which is clearly less extended distally than the caudal ridge, with the angle being either slightly (D2 extrem) or significantly greater (D2 typical) than 10°.

The last character (E) concerns a protuberance on the distal portion of the *os metacarpale majus* in dorsal view. In state 1, a clear protuberance is present in the extension of the caudal ridge limiting the *sulcus tendineus* (E1 typical) or only extends partially on the dorsal surface beyond the relief formed by the crest of the distal articulation (E1 extrem). In state 2, this protuberance is either absent (E2 typical) or cannot be differentiated from surface irregularities but is still clearly distinguishable from state 1 (E2 extrem).

Several characters identified in the modern sample (***Table 3***) reliably distinguish the different Mimidae species, particularly characters A and E, which separate *Mimus* from the other genera. Among specimens of the Antillean endemic clade, character B distinguishes *R. brachyurus* (B1 = 100%) from *D. carolinensis* (B2 = 80%). In the genus *Mimus*, state C2 is only absent in M. *gilvus*. *Allenia* is the only endemic species with a high frequency for C1 (88%), setting it apart from *D. carolinensis* and *C. ruficauda*. This latter species equally differs from *R. brachyurus* in character D (D1 = 80% for *C. ruficauda*, and D2 = 100% for *R. brachyurus*). Overall, several osteological characters are insignificant (<80%), and several species are represented by small sample sizes (e.g. *R. brachyurus* or *T. rufum*), suggesting caution in distinguishing Mimidae species based on osteology alone. With that said, several osteological characters nevertheless reliably discriminate members of the endemic genus *Mimus* as well as several endemic species of other genera. None of the specimens from our modern sample exhibits a co-occurrence of states A2 and E2.

Combining morphological characters with size data (***Table 3***) also produced more reliable results. *Margarops* and *Allenia* are distinguished by their large size and *Dumetella* is characterized by its small size, the other species have intermediate size.

GEOMETRIC MORPHOMETRIC ANALYSIS

Asymmetry in the right and left CMC was tested for *Allenia fusca*, the only Mimidae species for which enough specimens were available. A MANOVA performed on the first five PCA axes (representing respectively PC1*asym* = 29.2%, PC2*asym* = 11.2%, PC3*asym* = 10.3%, PC4*asym* = 8.1%, PC5*asym* = 7% of the total variance) showed no differences between left and right CMC (P = 0.201, Wilks' Lambda = 0.870). As such, both sides were combined in subsequent analyses. The lack of sex information makes it impossible to explore sexual dimorphism in the sample. Limited sexual dimorphism has, however, been previously reported for Mimidae species, especially for the endemic Caribbean mimids (Cody 2005).

Complete dataset

Centroid size analysis

Centroid size differences are significant between most species (***Figure 4***; ***Table 4***; Supplementary file 4). For taxa represented by a small number of individuals, these values potentially reflect only part of the variability and should be considered with caution. As mentioned above from traditional metric data, centroid size demonstrates *Margarops* to be the largest Mimidae species, followed by *Allenia*; *Dumetella* is the smallest. The centroid sizes of the other species overlap to different degrees, and a clear size gradient can be observed within the genus *Mimus*, with *M. gilvus* being the smallest, *M. polyglottos* intermediate in size, and *M. gundlachii* the

	A		B		C		D		E		METRIC	
SPECIES (N)	**A1**	**A2**	**B1**	**B2**	**C1**	**C2**	**D1**	**D2**	**E1**	**E2**	**GL (MM)**	**Bd (MM)**
C. ruficauda (5)	**100**	–	40	60	20	**80**	**80**	20	–	**100**	16,0 [15,3–16,9]	3,2 [3,1–3,3]
M. fuscatus (8)	**88**	12	25	75	50	50	62	38	–	**100**	22,7 [21,6–23,3]	4,5 [4,4–4,6]
A. fusca (16)	**100**	–	67*	33*	**88**	12	44	56	–	**100**	19,7 [19,1–20,4]	3,8 [3.6–4,0]
R. brachyurus (3)	**100****	–	**100**	–	33	67	–	**100**	–	**100**	15,7 [15,3–16,1]	3,1 [3,0–3,2]
D. carolinensis (5)	**100**	–	20	**80**	–	**100**	60	40	–	**100**	13,8 [13,4–14,2]	3,0 [2,9–3,1]
M. gilvus (4)	–	**100**	75	25	**100**	–	–	**100**	75	25	16,4 [15,9– 16,9]	3,3 [3,1–3,3]
M. polyglottos (6)	–	**100**	67	33	67	33	–	**100**	**100**	–	17,5 [16,2– 18,0]	3,5 [3,4– 3,7]
M. gundlachii (5)	–	**100**	60	40	60	40	–	**100**	**100**	–	18,6 [17,9– 19,1]	3,6 [3,4–3,6]
T. rufum (3)	**100**	–	33	67	33	67	–	**100**	–	**100**	16,8 [16,4– 17,4]	3,6 [3,6– 3,7]

Table 3 State frequency of the osteological character and metric data and in the modern specimens. (n) = number of specimens. Dominant characters (frequency ≥ 80%, in bold) reliably distinguish the Mimidae species. GL (Greatest Length of the CMC) and Bd (breadth of the distal end) are means calculated over n species. In brackets, the minimal and maximal values. * n observed = 15, ** n observed = 2.

largest. Pairwise differences between these species are significant. *Toxostoma rufum* appears similar in size to *Mimus* species, with no significant difference evident between *M. polyglottos* or *M. gilvus*.

Inter-group and inter-generic shape variation

The pan-continental and Antillean endemics clades are clearly set apart within the PC1-2 and PC2-3 morphospaces along PC2 (***Figure 5A*** and ***B***; Supplementary file 4). The first group clusters in the negative extreme of PC2, while the second group occupies the more positive extreme. This result is confirmed by a multivariate analysis of variance (MANOVA) performed on the first five axes ($P < 0.001$; Wilks' Lambda = 0.407). In particular, shape differences between the two clades reflect a more developed *facies articularis ulnocarpalis*, the dorsal portion of the *os metacarpale minus*, the *processus extensorius*, *processus intermetacarpalis*, *processus alularis*, and the cranial edge of the *sulcus tendineus* in species of the pan-continental clade, as can be seen along PC2 (***Figure 5F***). Shape changes associated with PC1 correspond to a more developed *trochlea carpalis*, *processus extensorius*, and *processus intermetacarpalis* (***Figure 5E***).

All genera included in the sample are also well differentiated (***Table 5***). Closely related taxa within each clade (***Figure 1***), such as *Mimus* and *Toxostoma*, or *Allenia* and *Cinclocerthia*, differ significantly along PC2 (***Figure 5***). *Allenia* and *Margarops* are also separated along PC1, although with some overlap. On the other hand, no separation between genera is evident in the PC3-4 morphospace, except for *Ramphocinclus*, which is distinct from the other specimens. Several specimens occupy extreme positions, a pattern which can be explained by their state of conservation. These specimens were nevertheless retained in the analysis due to the small sample sizes for certain species (i.e. *Cinclocerthia*: PACEA-O-846, *Margarops*: PACEA-O-826, *Dumetella*: NHMUK ZOO S/2010.2.15, *Ramphocinclus*: MNHN ZO 2012-550).

A classification matrix correctly predicted more than 60% of each Mimidae genus and more than 63% when species were represented by more than five individuals. Overall, the classification model attributed 84% of all specimens to the correct genus(***Table 6***).

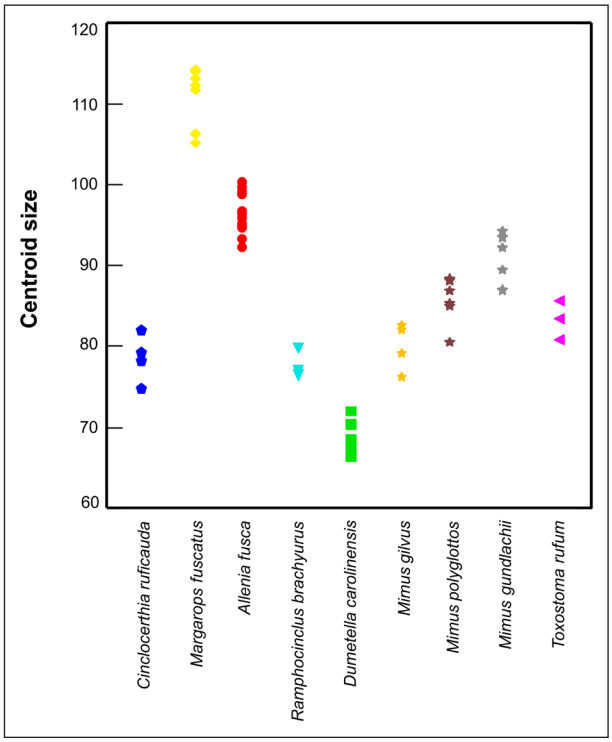

Figure 4 Variation in centroid size (CS) within the complete dataset. Species are organized by phylogenetic proximity (from left to right). Each dot represents a specimen. Symbol color reflects species, symbol shape refers to genus.

	C. RUFICAUDA	*M. FUSCATUS*	*A. FUSCA*	*R. BRACHYURUS*	*D. CAROLINENSIS*	*M. GILVUS*	*M. POLYGLOTTOS*	*M. GUNDLACHII*
M. fuscatus	**<0.001 *** **							
A. fusca	**<0.001 *** **	**<0.001 *** **						
R. brachyurus	0.68	**<0.001 *** **	**<0.001 *** **					
D. carolinensis	**<0.001 *** **	**<0.001 *** **	**<0.001 *** **	**0.001**				
M. gilvus	0.467	**<0.001 *** **	**<0.001 *** **	0.319	**<0.001 *** **			
M. polyglottos	**0.002 ** **	**<0.001 *** **	**<0.001 *** **	**0.004 ** **	**<0.001 *** **	**0.016 * **		
M. gundlachii	**<0.001 *** **	**<0.001 *** **	**0.001 ** **	**<0.001 *** **	**<0.001 *** **	**0.001 ** **	**0.012 * **	
T. rufum	**0.042 * **	**<0.001 *** **	**<0.001 *** **	**0.035 * **	**<0.001 *** **	0.173	0.253	**0.008 ** **

Table 4 Pairwise t-tests for Mimidae centroid size. Statistically significant values are in bold. (* = p-value comprise between 0.05 and 0.01; ** = p-value comprise between 0.05 and 0.01 and 0.001; *** = p-value inferior to 0.001).

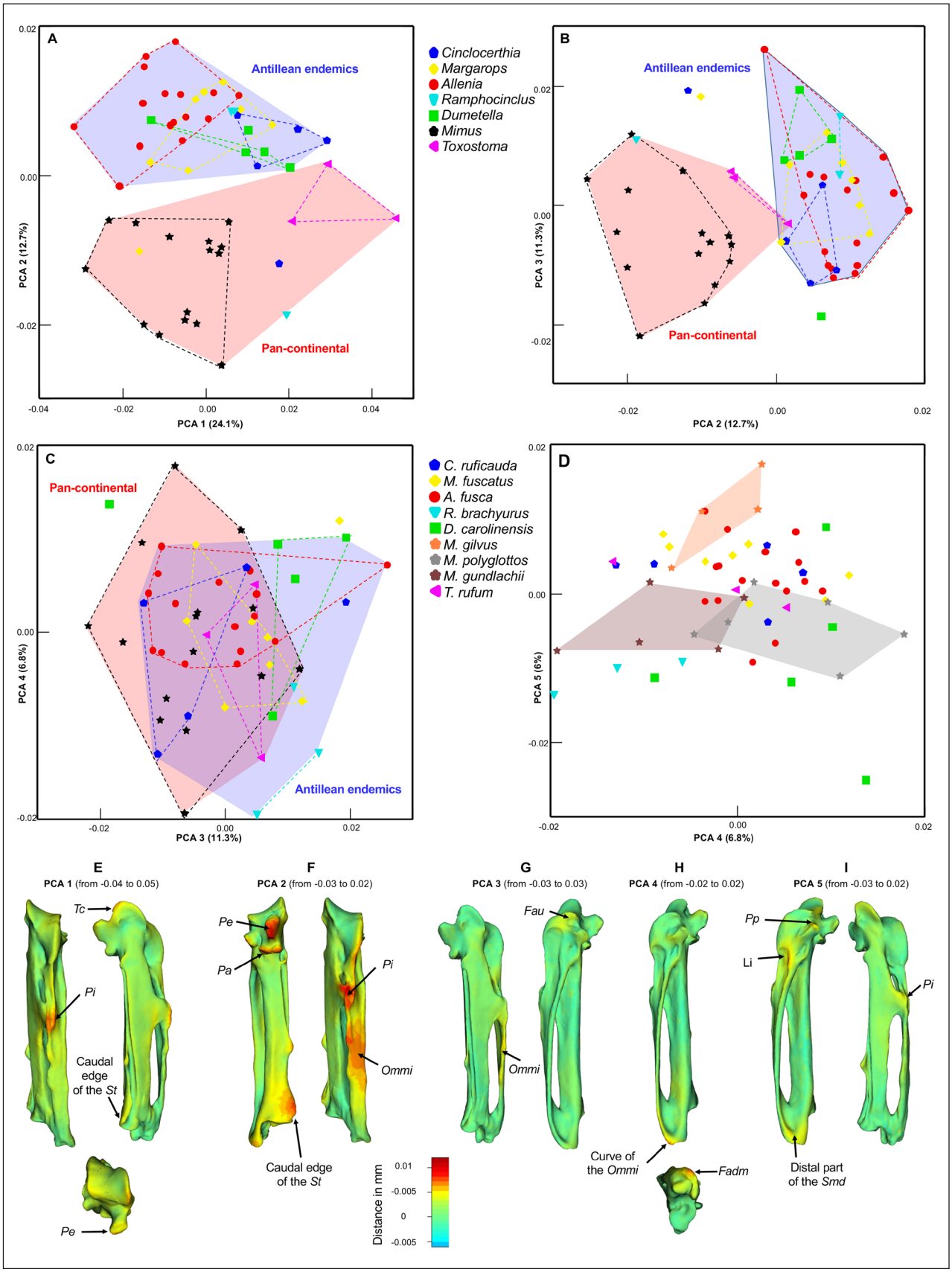

Figure 5 **A**, **B**, **C** and **D**: Principal Component Analysis (PCA) performed on all specimens. Each dot represents a specimen. Symbol colors represent species, while shapes reflect genus. The convex hull of each genus is outlined with dotted lines. The colored convex hulls represent Antillean endemics and Pan-continental genus. For **D,** the colored convex hulls represent the different species of *Mimus*. **E**-**F**-**G**-**H**-**I**: Distance map showing shape differences along axes 1 to 5, respectively. Views of the left CMC: E, cranial, dorsal and proximal; F, caudal and cranial; G, dorsal and ventral; H, ventral and distal; I, ventral and dorsal. Warm colors correspond to an expansion of the surface, cold colors to a compression. *Fadm*: *Facies articularis digitalis minor*; *Fau*; *Facies articularis ulnocarpalis*; *Li*: Ligament insertion; *Ommi*: *Os metacarpale minus*; *Pa*: *Processus alularis*; *Pe*: *Processus extensorius*; *Pi*: *Processus intermetacarpalis*; *Pp*: *Processus pisiformis*; Smd: *Symphysis metacarpalis distalis*; *St*: *Sulcus tendineus*; *Tc*: *Trochlea carpalis*.

	CINCLOCERTHIA	MARGAROPS	ALLENIA	RAMPHOCINCLUS	DUMETELLA	MIMUS
Margarops	**0.012 (0,168)**					
Allenia	**<0.001 (0,146)**	**0.043 (0,544)**				
Ramphocinclus	0.340 (0,153)	**0.003 (0,051)**	**<0.001 (0,066)**			
Dumetella	0.374 (0,358)	0.098 (0,325)	**0.001 (0,283)**	0.589 (0,299)		
Mimus	**0.007 (0,354)**	**<0.001 (0,204)**	**<0.001 (0,156)**	**0.001 (0,207)**	**0.001 (0,248)**	
Toxostoma	0.477 (0,228)	**0.007 (0,074)**	**<0.001 (0,090)**	0.704 (0,265)	0.496 (0,240)	**0.002 (0,247)**

Table 5 MANOVAs performed on the first five axes. The grouping variable is the genus. Significant *p*-values are in bold and Wilks' Lambda in brackets.

	CINCLO-CERTHIA	MAR-GAROPS	ALLENIA	RAMPHO-CINCLUS	DUMETELLA	MIMUS	TOXOSTOMA	CORRECT ATTRIBUTION (%)
Cinclocerthia	4	–	–	–	–	–	1	80
Margarops	1	5	2	–	–	–	–	63
Allenia	–	2	13	–	1	–	–	81
Ramphocinclus	–	–	–	3	–	–	–	100
Dumetella	–	1	–	1	3	–	–	60
Mimus	–	–	–	–	–	15	–	100
Toxostoma	–	–	–	–	–	–	3	100
Total	5	8	15	4	4	15	4	84

Table 6 Confusion matrix based on a linear discriminant analysis performed on the first five axes in the complete dataset.

Interspecific shape differences

Clear differences are evident in the PC4-5 morphospace of the three different *Mimus* species considered (***Figure 5D***). *M. gundlachii* differs from *M. polyglottos* along PC4 and is primarily due to a broader *processus extensorius* and *facies articularis digitalis minor* in *M. gundlachii* and a larger curvature of the *os metacarpale minus* (***Figure 5H***). The two sister-species, *M. polyglottos* and *M. gilvus*, segregate along PC5, reflecting a more developed *processus pisiformis*, the distal part of the *symphysis metacarpalis distalis*, a ligament insertion, and the *processus intermetacarpalis* (***Figure 5I***).

Distal dataset

Several specimens that plot at the extreme ends of the morphospace were excluded from the dataset when exploring size differences (*Cinclocerthia*: PACEA-O-846, *Margarops*: PACEA-O-826, *Dumetella*: NHMUK ZOO S/2010.2.15, *Ramphocinclus*: MNHN ZO 2012-550).

Centroid size analysis

Inter-species centroid size differences are still significant when the distal portion of the bone is considered alone (***Figure 6***; Supplementary file 5). For taxa with less than five specimens, tests are given as an indication and

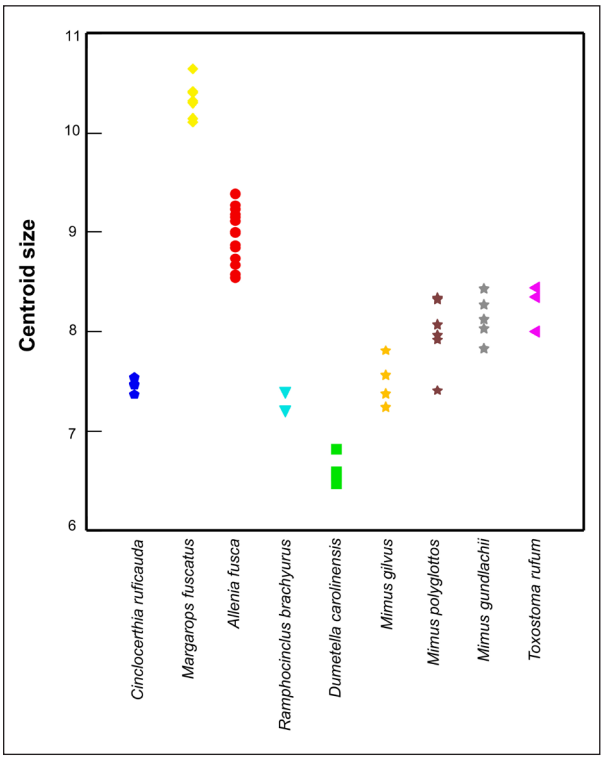

Figure 6 Variation in centroid size (CS) within the distal dataset. Species are organized by phylogenetic proximity (from left to right). Each dot represents a specimen. Symbol color reflects species, symbol shape refers to genus.

should be interpreted with caution. The same tendency can be observed as for the complete dataset: *Margarops fuscatus* is the largest species, followed by *Allenia fusca, and Dumetella* is the smallest. The same size ordering is observed in the whole dataset, apart from *M. gundlachii* (which is no longer distinct from *T. rufum* and *M. polyglottos),* and from *C. ruficauda* (which overlaps with the intermediate *Mimus* species *M. polyglottos*). Although the size gradient observed in the complete *Mimus* dataset is less clear, *M. gilvus* is still the smallest species while *M. polyglottos* and *M. gundlachii* overlap considerably.

Inter-genus shape variation

The separation between the pan-continental and Antillean endemics clades observed in the complete dataset is less evident within the PC1-2 and PC2-3 morphospaces (***Figure 7A*** and ***7B***; Supplementary file 5). Several genera are, however, set apart along the second axis, including *Dumetella* and *Mimus*. *Cinclocerthia* and *Ramphocinclus* stand out from the other Antillean endemic genus along axis 2. *Allenia* and *Margarops* cluster together in the center of the morphospace. *Cinclocerthia* and *Dumetella*, which were not clearly differentiated by the complete dataset, now appear separated along PC2.

A classification matrix correctly predicted more than 50% for each gender of Mimidae, with a total correct attribution of 71% across all genera (***Table 7***), slightly less than when the complete dataset is considered.

APPLICATION TO THE FOSSIL RECORD

Osteological characters and metric

Our data indicate that identifying fossil Mimidae specimens to species based uniquely on osteological characters is unreliable (***Table 8***). Three fossils exhibit combined A2-E2 states, a character absent in the modern sample, and at least three species attributions are possible for several other specimens. More certain species attributions are, however, possible for some fossils when osteological characters are combined with a consideration of size differences. The AC3-2019-O-1438 and PGR6-2016-O-182

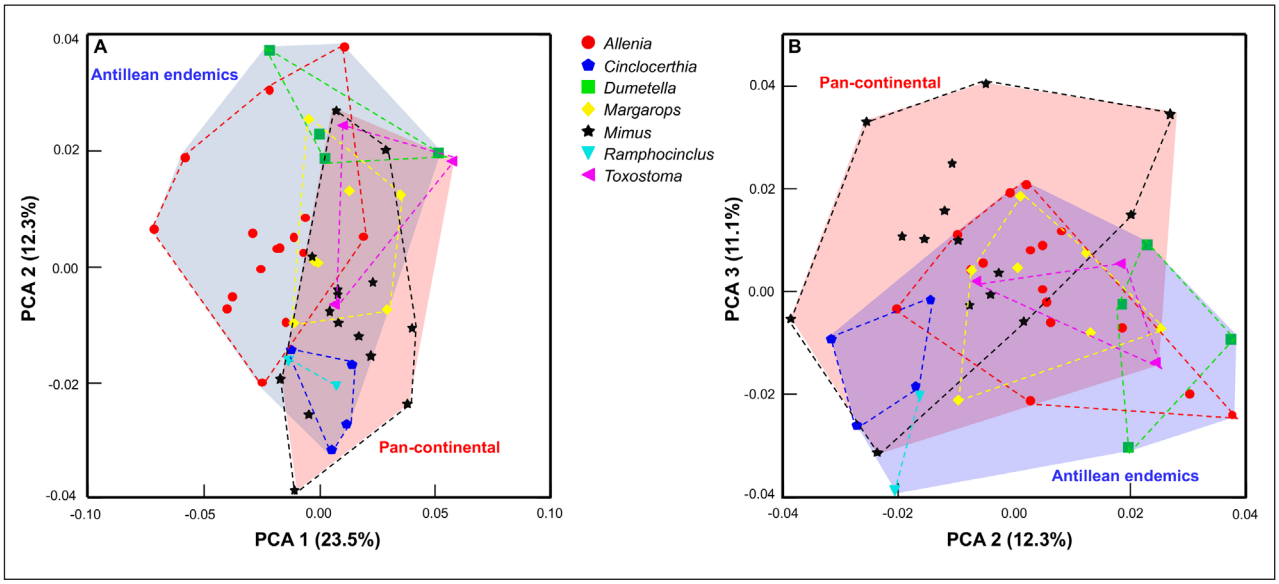

Figure 7 A and **B**: Principal Component Analysis (PCA) performed on all specimens (symbols) on the distal dataset. Each dot represents a specimen while their shapes refer to the genus. Dotted lines indicate the convex hull for each genus. Convex hulls for Antillean endemics are shown in blue, Pan-continental specimens in red.

	CINCLO-CERTHIA	MAR-GAROPS	ALLENIA	RAMPHO-CINCLUS	DUMETELLA	MIMUS	TOX-OSTOMA	CORRECT ATTRIBUTION (%)
Cinclocerthia	4	–	–	–	–	–	–	100
Margarops	–	5	–	–	–	2	–	71
Allenia	1	2	10	–	2	–	1	63
Ramphocinclus	1	–	–	1	–	–	–	50
Dumetella	–	–	–	–	4	–	–	100
Mimus	–	3	1	–	1	10	–	67
Toxostoma	1	–	–	–	–	–	2	67
Total	7	10	11	1	7	12	3	71

Table 7 Confusion matrix for genera and species based on a linear discriminant analysis performed on the first five axes in the distal dataset.

SPECIMENS	CHARACTERS					METRIC		IDENTIFICATION	
	A	B	C	D	E	GL (MM)	Bd (MM)	CHARACTERS > 80%	METRIC
BAM-2014-O-20	A2	B2	C2	D1	E2	14.7*	3,1		Cr, Rb, Dc, [Mgi]
AC3-2019-O-1435	A1	B2	C2	D2	E2	nm	3	Cr, Mf, Dc, Tr	[Rb, Dc, Mgi]
GB-2008-O-349	A1	B1	C2	D2	E2	18,7	4,1	Cr, Mf, Dc, Rb, Tr	Af, [Mgu]
GB-2008-O-361	A1	nc	nc	D2	E2	15,3	3,1	Cr, Mf, Af, Dc, Rb, Tr	Cr, Rb, [Dc, Mgi]
GB-2014-O-35	A1	B1	C1	D1	E2	16	3,3	Cr, Mf, Af	Cr, Rb, Mgi, Mp, [Dc, Mgu, Tr]
GB-2014-O-92	nc	B1	nc	D2	E2	18,6	4,1	Cr, Mf, Af, Dc, Rb, Mgi, Tr	Af, [Mgu]
GB-2014-O-156	A1	B1	C1	D1	E2	16,5	3,4	Cr, Mf, Af	Cr, Rb, Mgi, Mp, Tr, [Mgu, Af]
GC2-2014-O-1	A2	B2	C2	D1	E2	15,9	3,3		Cr, Rb, Mgi, Mp, [Dc, Mgu, Tr]
GC2-2014-O-2	A1	B2	C1	D2	E2	19,8	4,1	Cr, Mf, Af, Tr	Af
PGR6-2011-O-16	A2	B1	C2	D1	E2	14,9	3,2		Cr, Rb, [Dc, Mgi, Mp, Mgu]
PGR6-2011-O51	A1 extrem	B1	C1	nc	E2	15	3,4	Cr, Mf, Af, Rb, Tr	Cr, Rb, [Af, Mgi, Mp, Mgu, Tr]
PGR6-2016-O-182	A1	B1	C2	D1	E2	14,2	3	Cr, Mf, Dc	Dc, [Cr, Rb, Mgi]

Table 8 Osteological characters and metric data for the identification of fossil specimens. nc: non-observable. nm: non-measurable. *: broken but still measurable. In brackets, values that fit only with GL or Bd. Af = *Allenia fusca*; Cr = *Cinclocerthia ruficauda*; Dc = *Dumetella carolinensis*; Mf = *Margarops fuscatus*; Mgi = *Mimus gilvus*; Mgu = *Mimus gundlachii*; Mp = *Mimus polyglottos*; Rb = *Ramphocinclus brachyurus*; Tr = *Toxostoma rufum*.

specimens were both attributed to *D. carolinensis*. Osteological characters and size data suggest *A. fusca* for GB-2014-O-92 and GC2-2014-O-2 and *C. ruficauda* for GB-2014-O-35 and GB-2014-O-156. Specimens GB-2008-O-361 and PGR6-2011-O51 may represent either *C. ruficauda* or *R. brachyurus*. GB-2008-O-349 is the only specimen with substantially different species attributions based on osteological characters compared to metric data.

Species attributions based on the complete dataset

The centroid size (***Figure 8***) for GC2-2014-O-2 is similar to *Allenia* and approaches the highest values for *M. gundlachii*. GC2-2014-O-1 is comparable with *Cinclocerthia*, *Ramphocinclus* and *M. gilvus* while GB-2014-O-156 is similar with *Cinclocerthia* and *M. gilvus*. The specimen from PGR6 has a centroid size compatible with both *Dumetella* and *Cinclocerthia*.

The four complete archaeological specimens were plotted against the PCA of the reference dataset (***Figure 9***). PGR6-2011-O-51 falls outside the range of variation of the different species sampled in our study except along PC1-2, where it fits within the morphospace of *Allenia* (***Figure 9A***). GC2-2014-O-1 plots with the pan-continental group, close to the convex hulls of *Mimus* in the PC1-2 and PC2-3 morphospaces. The situation is less clear for GC2-2014-O-2, as it falls between the pan-continental and Antillean clades (***Figure 9A*** and ***9B***). GB-2014-O-156 is associated with the Antillean clade, plotting close to *Cinclocerthia*, *Margarops*, *Dumetella*, and *Allenia* (***Figure 9B***).

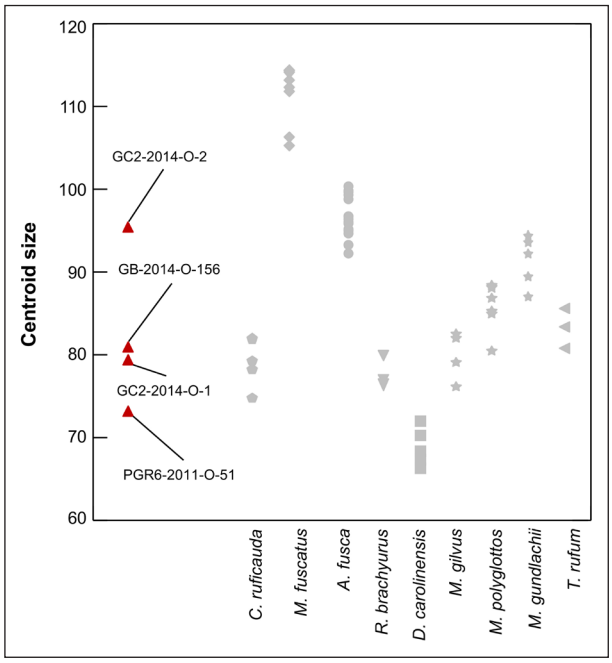

Figure 8 Centroid size of fossils specimens in the complete dataset. Modern species (grey symbols) are classified by phylogenetic proximity (from left to right). Symbols refer to genus. The fossils are presented by their reference number.

A phenogram performed on the first five PC scores places specimen PGR6-2011-O-51 at the base of the tree, separating it from the branches of modern specimens (***Figure 10***). Conversely, GC2-2014-O-1 clusters near *Cinclocerthia* while GC2-2014-O-2 and GB-2014-O-156 are grouped with *Dumetella*.

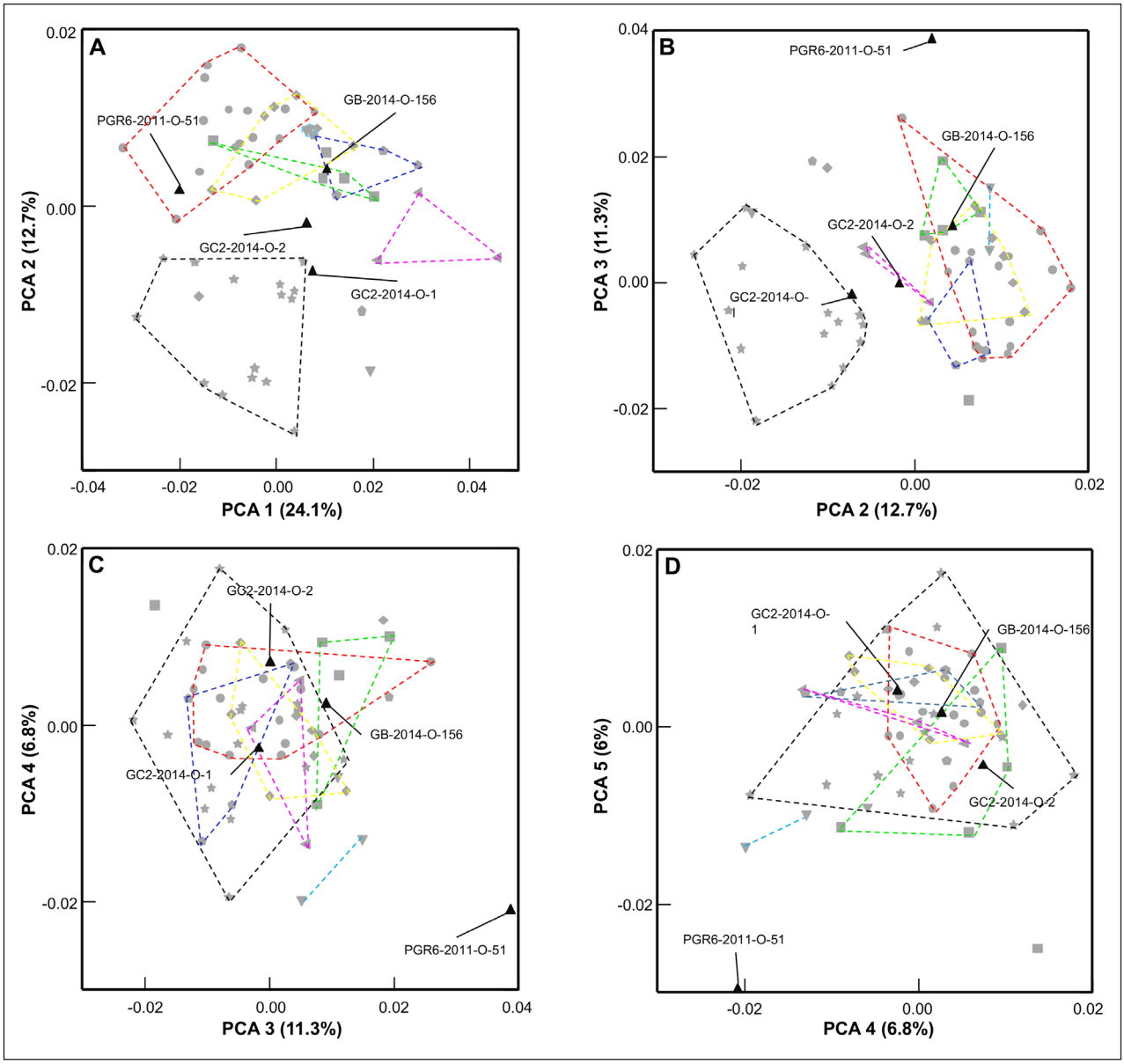

Figure 9 **A, B, C** and **D**: Principal Component Analysis (PCA) performed on all specimens (symbols) of the complete dataset. Each dot corresponds to an individual specimen, symbols represent genus. Convex hulls for modern specimens (in grey) are indicated by dotted lines (red: *Allenia*; yellow: *Margarops*; green: *Dumetella*; black: *Mimus*; dark blue: *Cinclocerthia*; light blue: *Ramphocinclus* and pink: *Toxostoma*). The extreme modern specimens were excluded from the convex hulls. Fossils specimens (in black) are indicated by their reference number.

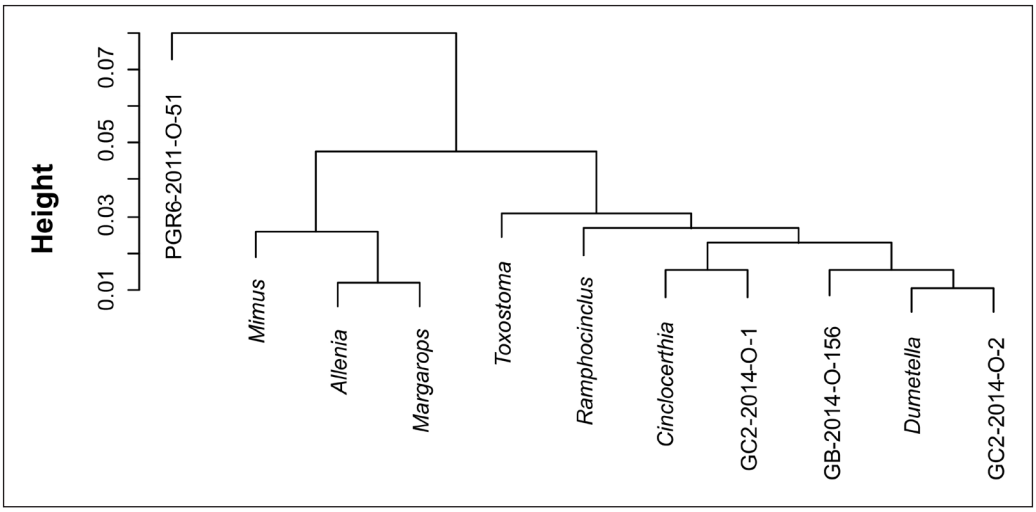

Figure 10 Phenogram of the complete dataset based on a matrix of Euclidean distances calculated between the means of the different groups using Ward's method (the first five axes of the PCA were considered).

Species attribution based on the distal dataset

The centroid size for all PGR6 specimens falls between the genus *Cinclocerthia* and *Ramphocinclus* and the smaller *M. gilvus* (***Figure 11***). The smallest of the PGR6 specimens is also close to *Dumetella*. Two size groups can be distinguished amongst the *Grotte Blanchard* specimens: one with small centroid size consistent with *Mimus* species and larger individuals of *Cinclocerthia* and *Ramphocinclus,* the other with larger centroid size compatible with *Allenia*. The centroid size of GC2-2014-O-2 falls between those of *Allenia* and *Margarops*, and GC2-2014-O-1 presents a centroid size similar in size to that of *Ramphocinclus*, *Cinclocerthia*, and *M. gilvus*.

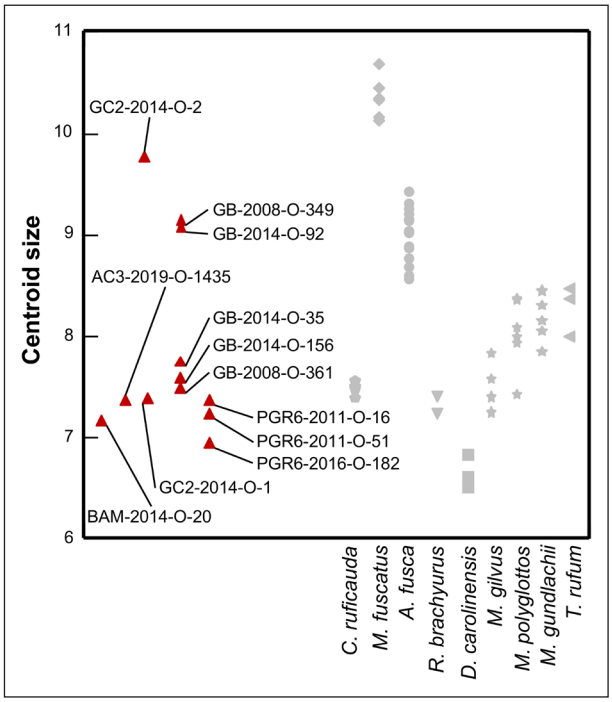

Figure 11 Centroid size for Mimidae species in the distal dataset. The modern species (in grey) are classified by phylogenetic proximity (from left to right). Symbols refer to the genus. The fossils (in brown) are classified by geographic origin (from left to right): Grande-Terre (Grotte des Bambous specimen), Marie-Galante (GC and GB specimens) and La Désirade (PGR6 specimens). Fossils specimens are indicated by their reference number.

The fossils were projected on the PCA run for the distal dataset (***Figure 12***). When the first five PC scores are plotted, the distinction between several genera is not evident, while others, such as *Cinclocerthia* and *Ramphocinclus*, are clearly distinct from other modern specimens within the PC1-2, PC2-3, PC3-4, and PC2-4 morphospaces. A MANOVA reveals fewer significant differences than for the complete dataset, with the exception of *Allenia* and *Mimus* (***Table 9***). Fossils from PGR6 tend to group together near the ranges of *Cinclocerthia* and *Ramphocinclus* in all morphospaces. Specimens from *Grotte Blanchard* also group together close to the ranges of *Margarops*, *Mimus* and *Allenia*. The *Grotte des Bambous* fossil does not plot within a particular morphospace of the modern specimens but falls within or relatively close to the range of *Margarops,* depending on the PC axis considered. AC3-2019-O-1435 fits within the morphospace of *Allenia* in all PC morphospaces except PC3-4. GC2-2014-O-1 plots close to within the range of *Cinclocerthia* (cf. PC2-3 and PC3-4), while GC2-2014-O-2 falls within the range of *Allenia* for all PC.

A phenogram performed on the first five axes of the distal dataset (***Figure 13***) confirms the PGR6 specimens to cluster with the genus *Ramphocinclus* and *Cinclocerthia*. GC2-2014-O-1 occupies the basal branch of *Cinclocerthia* and *Ramphocinclus*. GC2-2014-O-2 and AC3-2019-O-1435 fit with *Allenia* and GB-2008-O-361 occupies the basal branch of *Allenia*. The specimen from *Grotte des Bambous* fits with *Margarops,* and, apart from GB-2008-O-361, the *Grotte Blanchard* fossils are positioned close to *Margarops* and *Mimus*.

SYNTHESIS

Species attributions based on traditional osteological characters (***Table 8***) and geometric morphometrics (***Table 10***) for complete CMC (***Figure 14***) and the distal portion of this bone (***Figure 15***) are combined in a single table.

	CINCLOCERTHIA	*MARGAROPS*	*ALLENIA*	*RAMPHOCINCLUS*	*DUMETELLA*	*MIMUS*
Margarops	0.123 (0.247)					
Allenia	**<0.001 (0.216)**	**<0.001 (0.293)**				
Ramphocinclus	0.346 (0.055)	0.333 (0.250)	**0.001 (0.228)**			
Dumetella	**0.085 (0.035)**	**0.031 (0.135)**	0.110 (0.557)	0.122 (0.007)		
Mimus	**0.003 (0.292)**	0.377 (0.736)	**<0.001 (0.304)**	**0.004 (0.245)**	**0.001 (0.247)**	
Toxostoma	0.595 (0.142)	0.117 (0.180)	0.133 (0.555)	0.398 (0.101)	0.479 (0.087)	**0.003 (0.264)**

Table 9 MANOVAs performed on the first five axes of the different genera. Significant *p*-values are in bold and Wilks' Lambda is in brackets.

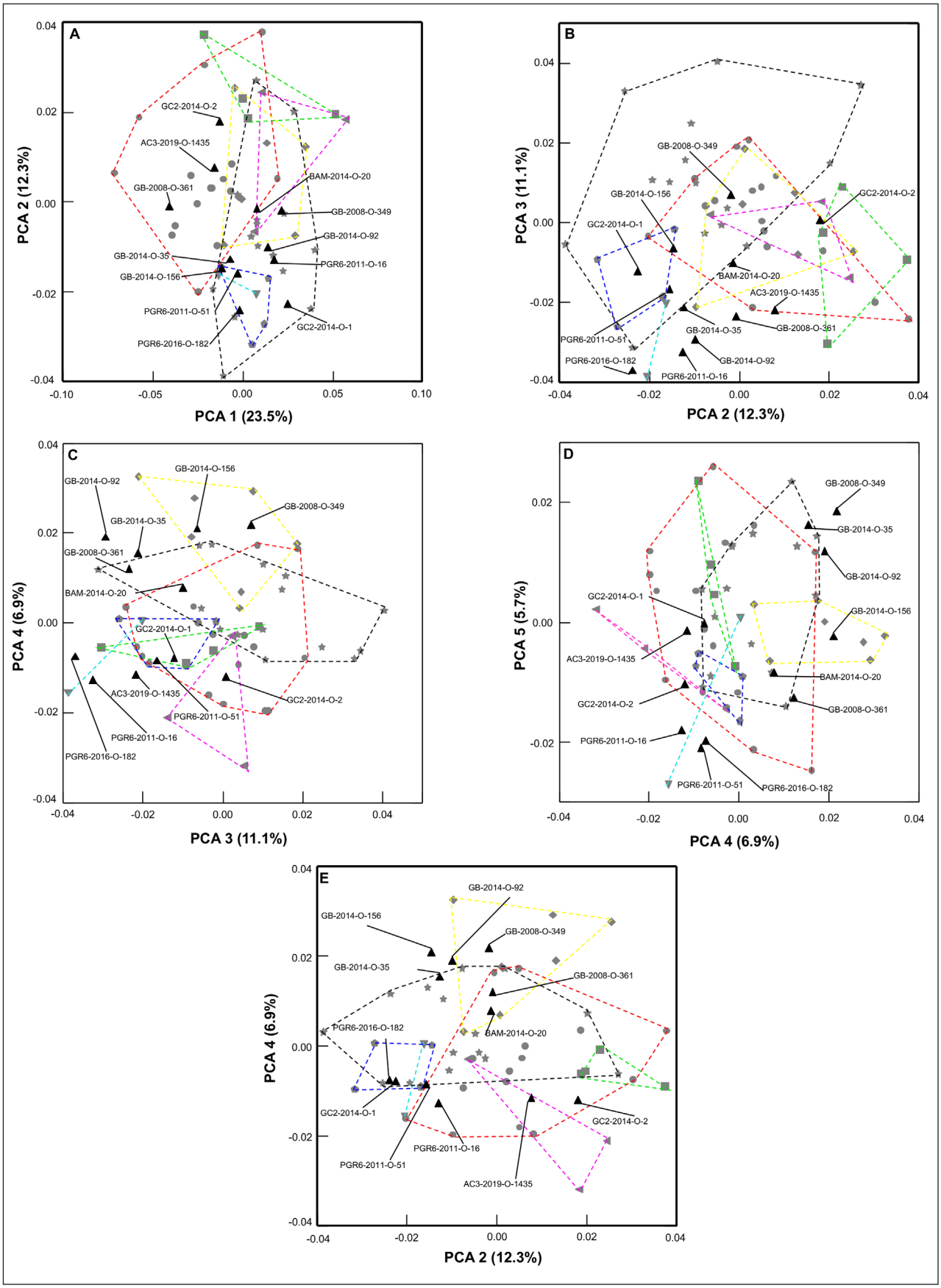

Figure 12 **A**, **B**, **C**, **D** and **E**: Principal Component Analysis (PCA) performed on all specimens (symbols) of the distal dataset. Each dot corresponds to an individual while the symbols represent the genus. Convex hulls for modern specimens (in grey) are indicated by dotted lines (red: *Allenia*; yellow: *Margarops*; green: *Dumetella*; black: *Mimus*; dark blue: *Cinclocerthia*; light blue: *Ramphocinclus* and pink: *Toxostoma*). The fossils are indicated by their reference number.

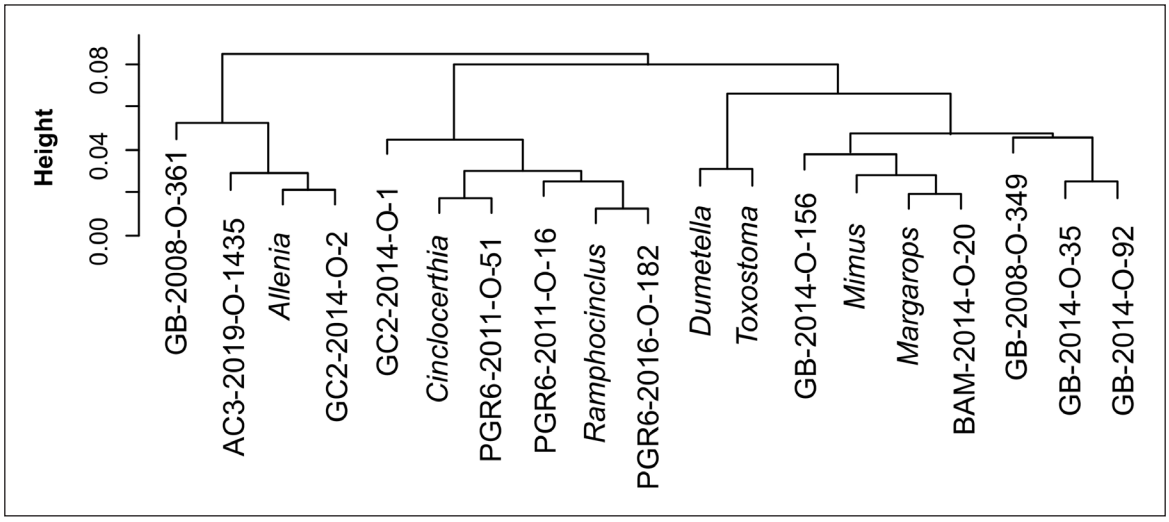

Figure 13 Phenogram based on a matrix of Euclidean distances calculated between the means group and the first five axes of the PCA run for the distal dataset.

	COMPLETE DATASET			DISTAL DATASET		
SPECIMENS	**MATRIX CLASSIFICATION (%)**	**PHENOGRAM**	**CENTROID SIZE**	**MATRIX CLASSIFICATION (%)**	**PHENOGRAM**	**CENTROID SIZE**
BAM-2014-O-20	–	–	–	Cr (24%), Mf (32%), Af (10%), *Mimus sp.* (26%)	Mf	[Cr], [Rb], [Dc], [Mgi], [Mp]
AC3-2019-O-1435	–	–	–	Af (56%), Dc (12%)	Af	Rb, Mgi, [Cr], [Mp], [Mgu]
GB-2008-O-349	–	–	–	Mf (71%), *Mimus sp.* (28%)	–	Af
GB-2008-O-361	–	–	–	Cr (16%), Af (52%),	Af	Cr, Mgi, Mp, [Rb], [Mgu]
GB-2014-O-35	–	–	–	Mf (52%), *Mimus sp.* (37%)	–	Mgi, Mp, [Cr], [Rb], [Mgu], [Tr]
GB-2014-O-92	–	–	–	Mf (75%), *Mimus sp.* (20%)	–	Af
GB-2014-O-156	Cr (29%), Mf (36%), Dc (32%)	Dc	Cr, Mgi, Mp, Tr, [Rb]	Mf (11%), *Mimus sp.* (24%)	Mf, *Mimus sp.*	Mgi, Mp, [Cr], [Rb], [Mgu], [Tr]
GC2-2014-O-1	Cr (50%), *Mimus sp.* (39%)	Cr	Cr, Rb, Mgi, [Mp], [Tr]	Cr (79%)	Cr, Rb	Rb, Mgi, [Cr], [Mp], [Mgu]
GC2-2014-O-2	Cr (25%), Mf (20%), Dc (50%)	Dc	Af, [Mgu]	Af (58%) Dc (15%)	Af	[Mf], [Af]
PGR6-2011-O-16	–	–	–	Cr (18%)	Rb	Rb, Mgi, [Cr], [Mp], [Mgu]
PGR6-2011-O51	–	–	[Cr], [Rb], [Dc], [Mgi]	Cr (37%)	Cr	Rb, [Cr], [Dc], [Mgi], [Mp]
PGR6-2016-O-182	–	–	–	Cr (12%)	Rb	[Cr], [Rb], [Dc], [Mgi], [Mp]

Table 10 Synthesis of fossil attributions based on morphology. CS + 0.5 or – 0.5 of the minimum and maximum value of current species are in brackets. The matrix classification column presents the probability of a fossil being attributed to a current species. Af = *Allenia fusca*; Cr = *Cinclocerthia ruficauda*; Dc = *Dumetella carolinensis*; Mf = *Margarops fuscatus*; Mgi = *Mimus gilvus*; Mgu = *Mimus gundlachii*; Mp = *Mimus polyglottos*; Rb = *Ramphocinclus brachyurus*; Tr = *Toxostoma rufum*.

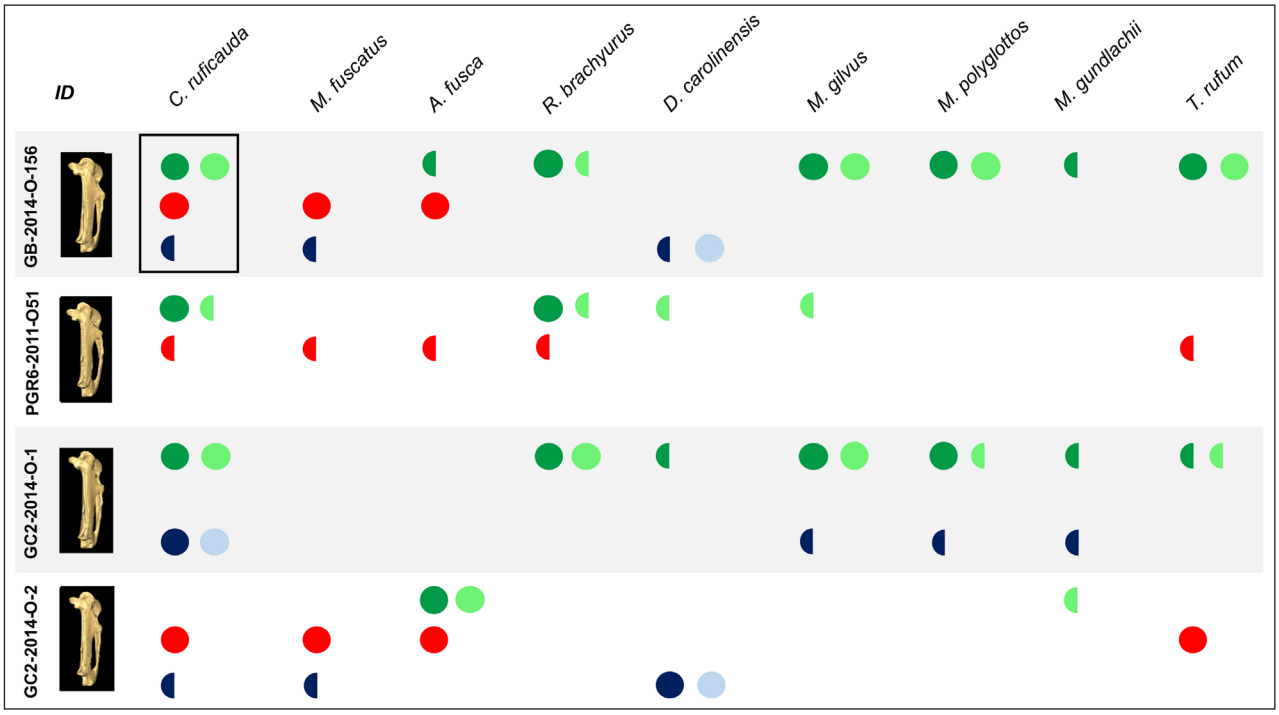

Figure 14 Synthesis of fossil attribution based on osteological and morphometric geometric data using the complete dataset. An attribution is proposed (boxed in black) when at least 3 colors are present. Criteria are: **Size** (conventional: dark green circles or CS: light green circles). For conventional, filled circles represent values between the minimum and maximum for each species (GL + Bd) and half sticker when value is only on GL or Bd. For CS, full circles indicate values between the minimum and maximum for each species and half circles when the value is + or – 0.5 of the minimum and maximum value of one species. **Osteological characters**: red circles. Half circles when 3 or 4 characters out of 5 are present. **Matrix reclassification** (or probability): dark blue circles. Half circles when probability <50%. **Phenogram**: light blue circles.

Two different size groups are evident in the *Grotte Blanchard* and *Grotte Cadet 2* fossils. While the large specimen GC2-2014-O-2 cannot be attributed to a particular species based on the complete dataset, its size (conventional and CS) and osteology are compatible with *A. fusca*, an attribution equally supported by both approaches to the distal dataset.

The large fossils GB-2008-O-349 and GB-2014-O-92 are also impossible to unambiguously attribute to a particular species due to diverging results for the different methods. For the first specimen, its osteology and position close to the convex hull of *M. fuscatus* in morphospaces 3–4 and 4–2 are consistent with *M. fuscatus* and, while the second presents the same traits, its morphometry is less certain due to slight damage affecting parts of the bones. However, the two fossils are smaller than *M. fuscatus* but similar in size to *A. fusca*, making it compatible with both species.

In terms of the smaller fossils, both datasets attribute GC2-2014-O-1 to *C. ruficauda* based on both its size and geometric morphometric criteria. Although this specimen displays the combination of states A2-E2 which is absent in the modern sample, the highly pronounced proximal concavity of the cranial edge is typical of modern specimens of *C. ruficauda*, which argues in favor of referring the fossil specimen to this species.

The position of BAM-2014-O-20 falls within several convex hulls, however its size and morphometry are compatible with *C. ruficauda* or *M. gilvus*. Like the previous individual, this specimen presents both the combination of states A2 and E2 and a highly pronounced proximal concavity, suggesting *C. ruficauda* for attribution.

Both GB-2008-O-361 and GB-2014-O-156 are referred to *C. ruficauda* based on the distal and complete dataset, respectively. The distal dataset does not allow GB-2014-O-156 to be attributed to a species, although the specimen's osteological characters and size are compatible with *C. ruficauda*. GB-2014-O-35, while morphologically similar to *M. fuscatus* (based on the GMM), its small size is incompatible with this species. Moreover, the specimen plots close to *C. ruficauda* in morphospaces 1–2 and 2–3, a potential attribution equally supported by its size and osteology. Finally, this fossil specimen is similar to the previous two, suggesting it belongs to the same taxon.

The three fossils from PGR6 cluster together in the PCAs (***Figure 12***). Of these three specimens, PGR6-2011-O51 and PGR6-2016-O-182 can be reliably attributed to *C. ruficauda* based on a good fit between size, morphological characters and morphometric geometric criteria of the distal CMC (***Figure 15***). PGR6-2011-O-16 associates only size and geometric morphometric criteria, both of which are compatible with *C. ruficauda* and *R. brachyurus*. However, its proximity in the PCA to the two previous fossils may suggest it belongs to *C. ruficauda*.

Multiple characters and its position in the PCA identify specimen AC3-2019-O-1435 as *D. carolinensis*.

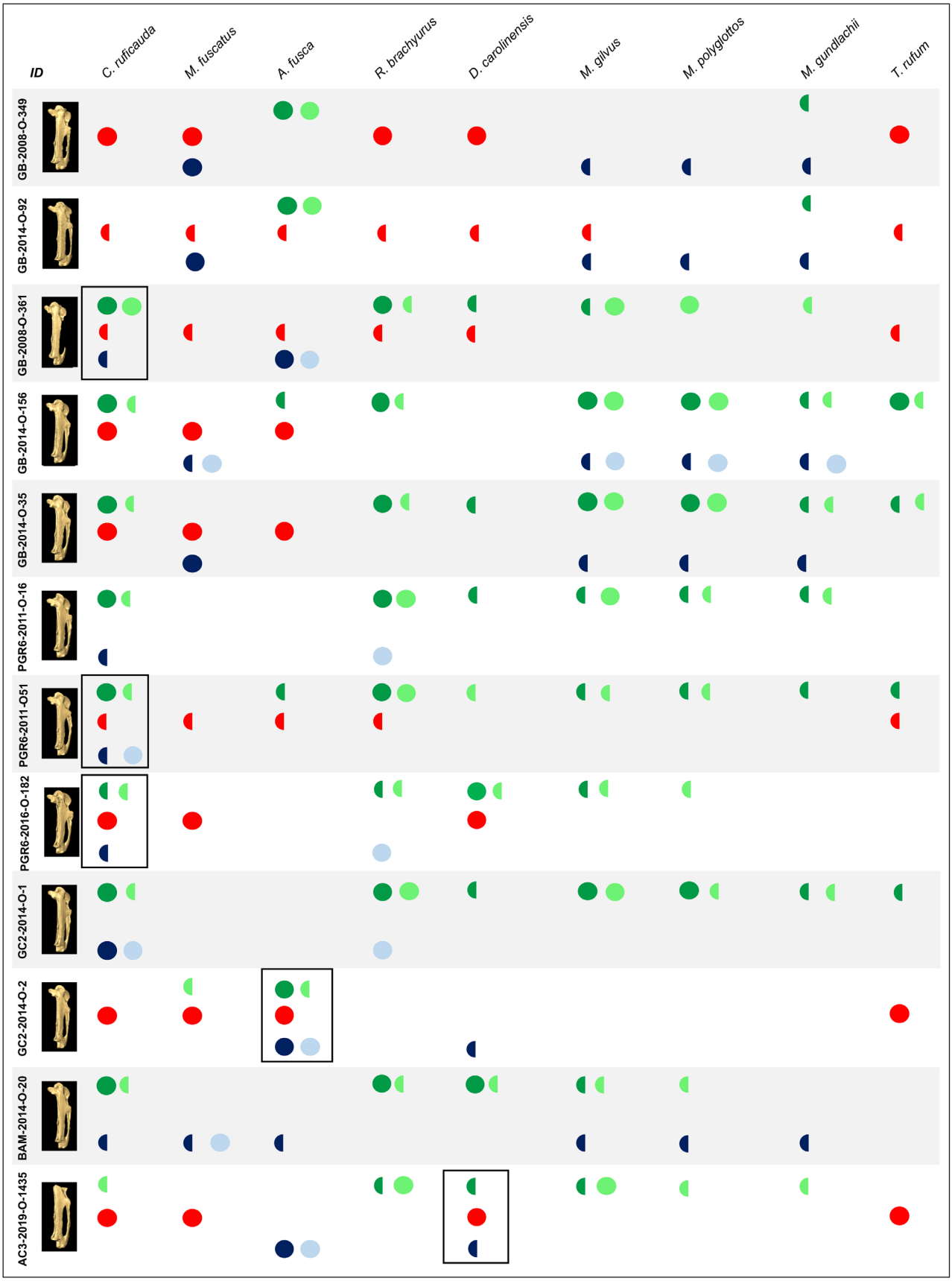

Figure 15 Synthesis of fossil attribution based on osteological and morphometric geometric data using the distal dataset. An attribution is proposed (boxed in black) when at least 3 colors are present. Criteria are: **Size** (conventional: dark green circles or CS: light green circles). For conventional, filled circles represent values between the minimum and maximum for each species (GL + Bd) and half sticker when value is only on GL or Bd. For CS, full circles indicate values between the minimum and maximum for each species and half circles when the value is + or – 0.5 of the minimum and maximum value of one species. **Osteological characters**: red circles. Half circles when 3 or 4 characters out of 5 are present. **Matrix reclassification** (or probability): dark blue circles. Half circles when probability <50%. **Phenogram**: light blue circles.

DISCUSSION

A DEDICATED METHODOLOGY

Here we propose a dedicated methodology that combines geometric morphometrics and conventional osteology mobilizing both character-state coding and metric data, on the one hand, and a focus on both the complete carpometacarpus as well as the distal portion of this bone, on the other hand. This multi-evidence methodology is particularly suited to characterizing passerine osteology, as this order of birds comprises families with numerous members that display limited osteological differences between them (Moreno 1985; Mourer-Chauviré 1975).

Damaged bones outnumber complete examples in our fossil sample, which is likely a common preservation pattern for bird remains, past and present. Integrating damaged specimens with preserved distal portions in analyses not only increases the number of fossil specimens but also enhances our capacity to document past biodiversity in avian communities.

The results obtained from the GMM analyses between distal part and whole bone may differ. The anatomical features present on the distal portion of the CMC depict only part of the total variance of the complete bone. When only the distal portion is considered, this variance is determinant and may produce different results in the GMM analysis. This effect is exemplified by specimen GC2-2014-O-2, which is attributed by the confusion matrix to *D. carolinensis* based on the complete bone or *A. fusca* based on the distal portion. When additional data is combined in the analysis, in this case character coding, metrics, and GMM, the specimen in question can be reliably attributed to *A. fusca*. Combining different approaches can therefore help resolve conflicting results based on a single analytical approach. In several cases, however, species attributions vary between methods, as is the case for GB-2014-0-156. Fossil specimens could be reliably determined to species by combining results from the whole bone and its distal portion while working with the assumption that specimens from the same site that share a very similar morphology and size represent the same population. Classical osteology successfully isolated new species-specific features. In addition, it can easily be applied to damaged bones. With that said its utility for determining Mimidae is limited, as each species from this family does not exhibit an exclusive combination of characters. Geometric morphometrics, on the other hand, provides an analytical framework supported by multivariate statistics that allows differences between taxa to be tested and visualized, either as averaged conformations for different populations or along principal component axes. Consequently, similarities and differences between taxa and fossil specimens can be appreciated at a finer scale than is possible with other more traditional approaches. Finally, forest birds show a well-expressed size differentiation in response to competitive exclusion, especially in the Caribbean area (Case, Faaborg & Sidell 1983), making size an important factor for determining specimen to species. Paradoxically, this situation makes size a time sensitive character connected to the species-level composition of the avian community. As such, this data should be treated with caution when considering fossil material (e.g., Stewart 2007).

Finally, despite concerted efforts to assemble a large set of modern specimens, many species are represented by a very limited number of individuals, a difficulty well known for Caribbean flying vertebrate species, with most of them being rare, endangered and under-represented in museum collections (e.g. Lefevbre & Sharpe 2018; Lenoble, Gala & Laroulandie 2019; Steadman & Franklin 2017). A larger sample would potentially increase the reliability of these results by more accurately evaluating the frequency of character states.

PHYLOGENETIC HISTORY AS A KEY FACTOR INFLUENCING CARPOMETACARPUS SHAPE VARIATION

The North American origin of the Mimidae family is now well established (Arbogast et al. 2006; Bond 1948, 1963; Lovette et al. 2012), with the wide geographic distribution of the genus *Mimus* seeming to have a higher colonizing potential compared to endemic Mimidae species of the Lesser Antilles. *M. polyglottos* colonized the Lesser Antilles 0.3 Ma ago (Aldridge 1984; Hunt, Bermingham & Ricklefs 2001), *M. gilvus* between 0.4 and 0.6 Ma *via* South-America (Bond 1963; Hunt, Bermingham & Ricklefs 2001), and *M. gundlachii* currently occurs in the Bahamas but has been reported in Jamaica (Cody 2005; Hunt, Bermingham & Ricklefs 2001; Raffaele 2003). Lovette and colleagues (2012) propose that Mimidae of the Lesser Antilles have a complex pattern of island occupation, including the sympatric occupation of Martinique by all Antillean Mimidae species (*Cinclocerthia*, *Ramphocinclus*, *Allenia* and *Margarops*). Natural barriers (e.g. middle mountains, distance between islands) and the multiple habitats of the Caribbean islands would favor the isolation of species, leading to the appearance of morphological or behavioral differences, as previously discussed for Amazonian passerines (Hayes & Sewlal 2004).

Phylogeny nevertheless appears to play a primary role in explaining CMC shape. Our results reveal high evolvability of this anatomical element between Mimidae species. Similarities between the morphological and phylogenetic signature equally raises questions concerning the impact of population history. The two previously identified Antillean and pan-continental Mimidae clades based on genetic analyses (Lovette and Rubenstein 2007; Lovette et al. 2012; DaCosta et al. 2019) are equally evident in the morphometric analysis

of the complete dataset. The morphological similarity between species of Antillean clade is not surprising given their geographical proximity. The same trend is also exhibited at the interspecific level between two members of the genus *Mimus*: *M. gilvus* and *M. polyglottos*. While these taxa have been observed to hybridize along their contact zone in central Mexico (Wetmore 1943), the precise relationships between these two species remains complex and not fully understood. The results of the PCA analysis (***Figure 5D***) are in good agreement with the mtDNA analysis (Hunt, Bermingham & Ricklefs 2001) that suggested these taxa to be clearly distinct and to differ from *M. gundlachii* (Arbogast et al. 2006).

CHANGES IN FOREST BIRD COMMUNITIES

Our analysis of a dozen CMC from archaeological and paleontological deposits in the Guadeloupe Islands identified three fossil taxa, *Cinclocerthia ruficauda*, *Dumetella carolinensis*, *Allenia fusca*, which likely represent only a portion of this region's past avifauna. The eventual integration of additional material from these types of contexts may broaden our vision of the islands' past biodiversity. For example, 11 bird taxa were reported from the mid-Holocene Burma Quarry site on the neighbouring island of Antigua. Four taxa were identified based on descriptions of the CMC, the rest using the tarsometatarsus and the tibiotarsus (Pregill et al. 1988). Despite the fact that limb bones are often heavily fragmented, complete and slightly damaged CMC nevertheless proved to have high taxonomic value.

Notwithstanding the limited number of taxa determined, our results document significant long-term diachronic changes in avian biogeography. The Scaly-breasted Thrasher identified from the late Pleistocene deposits of *Grotte Cadet 2* on Marie-Galante is perhaps the least interesting, as this bird is common on the different islands of Guadeloupe (Terborgh, Faaborg & Brockmann 1978; Bénito-Espinal & Hautcastel 2003). On the other hand, the Gray Catbird does not nest in the Caribbean but winters in the Bahamas and Greater Antilles (Cody 2005). This bird is rarely sighted in the islands of Guadeloupe (Levesque & Delcroix 2019) and has been observed only twice on La Désirade in the last fifteen years (Levesque, in litt.). The determination of a Grey Catbird bone from the *Abri Cadet 3* on Marie-Galante suggests this species had a larger wintering range that included the islands of Guadeloupe. This specimen was recovered from a level dating to between 3000 and 1000 years before present, a period that experienced climatic conditions similar to those at present (Curtis, Brenner & Hodell 2001). Consequently, the past presence of this species in the Lesser Antilles does not seem to reflect climatically-induced environmental change. The depletion of landbirds since the Holocene is well documented in the Greater Antilles (Orihuela et al. 2020) and the Bahamas (Steadman & Franklin 2020) and has been attributed to the impact of human activity in the archipelago. The past presence of the Grey Catbird on Marie-Galante and its current absence from the island could therefore be part of a regional extirpation phenomenon.

The most striking result of our study is the widespread presence of the Brown Trembler in the fossil record of the Guadeloupe islands, occurring in the Pleistocene on Marie-Galante, and in the Holocene on Désirade and, presumably, on the eastern coast of Grande Terre. This bird is currently absent from La Désirade and Marie-Galante (Terborgh, Faaborg & Brockmann 1978; Bénito-Espinal & Hautcastel, 2003; Levesque & Delcroix, 2021). While the Brown Trembler currently occurs on Grande Terre, its distribution is limited to the western part of the island, where it is essentially present in the littoral swamp forest (eBird, 2021). Its past presence at the *Grotte des Bambous*, on the eastern coast of this island, would therefore suggest a contraction in its range, even on the two main islands of Guadeloupe.

Today, the Brown Trembler is mainly found in the rain forest of the steep volcanic island of Basse Terre (Terborgh, Faaborg & Brockmann 1978). This situation is not peculiar to Guadeloupe, but is typical of the Lesser Antilles as a whole. This bird is mainly observed in the tropical rain forests on the slopes of the mountainous volcanic islands forming the inner arc and is absent from the dry, low-lying carbonate platforms on the islands of the outer volcanic arc which are covered by deciduous or dry scrub forest (Terborgh, Faaborg & Brockmann 1978). This species is also absent from the coastal areas of the wet islands, which are covered by dry or seasonal evergreen forest, at least during the dry season (Steadman et al. 1997; Zusi 1969). As such, the Brown Trembler is the only Mimidae species to show a preference for tropical rain forest (Cody 2005). The fossil specimens identified in this study, in contrast, depict a much wider range of past habitats occupied by this bird, including dry islands. Its presence in natural Pleistocene fossil-bearing deposits on Marie-Galante (Grotte Blanchard) excludes these specimens having been imported by humans. In addition, this is consistent with the report of Brown Trembler remains from Burma Quarry on the neighbouring island of Antigua (Pregill et al. 1988). Moreover, our comparative dataset includes all others dry forest-dwelling Caribbean Mimidae, ruling out the determination of the Brown Trembler as a misidentification of a distant species (Stewart 2005), above all the White-breasted Thrasher, which occurs in the dry coastal forests of St. Lucia and Martinique.

The Brown Trembler exhibits adaptations for arboreal feeding (Zusi 1969), namely a long, curved beak that enables it to probe Bromeliads for food (Storer 1989). These features led Pregill et al. (1988) to deduce that the presence of this species in Antigua reflected a well-structured, canopied forest coincident with the formation of the fossil deposit. This interpretation can

be extended to the dry islands of Guadeloupe, where the primary forest was decimated during the colonial era, first for wood and then for the cultivation of sugar cane. On La Désirade, a sharp reduction in environmental productivity is attributed to the impact of deforestation, subsequent agricultural activity and goat herding, which resulted in significant erosion of the soil. These human-induced environmental changes led to the collapse of the food web and the disappearance of the vertebrate species it supported (Boudadi-Maligne et al. 2016), this would include the extirpation of the Brown Trembler from the dry islands of the Lesser Antilles.

It should be noted that fossil remains of tremblers have been recovered from the *Grotte Blanchard* on Marie-Galante, in levels corresponding to the region's most arid period (Royer et al. 2017), as well as from the wetter pre-Columbian Holocene levels at La Désirade, thus both extremes of climatically-induced environmental variability. The perennial presence of tremblers on dry islands in the past suggests this bird to be highly resistant to climatically-induced environmental changes, whereas its recent disappearance indicates its sensitivity to human-induced changes to its habitats. This would be consistent with research supporting the primary role played by human activity in the loss of terrestrial vertebrates in the Caribbean (Cooke et al. 2017; Orihuela et al. 2020; Steadman & Franklin 2020).

Our analysis also revealed the currently available collection of modern osteological specimens to document only part of the past morphological variability of West Indian mimids. This can be observed in two ways. The first is the co-occurrence of two characters (A2-E2) on the proximal and distal portion of the CMC in three of the eight fossil specimens attributed to the brown trembler. This association is absent in the five modern specimens of the comparative sample and may reflect either the limited number of specimens, which only partially reflects the intra-specific osteological variability of the species, or greater variability of this species in the past. Second, it proved impossible to attribute the large Pleistocene Mimidae recovered from the *Grotte Blanchard* to any of the current members of this family. The similar morphological and size of the two fossil specimens strongly suggest that they belong to the same population. These two specimens are similar to the Scaly-breasted Thrasher both in size and conventional osteological characters, while the geometric morphometric analysis positions them closer to the Pearly-eyed Thrasher. It is difficult to attribute this non-congruence to a small number of Scaly-breasted thrashers in the comparison collection, as this taxon is represented by more than fifteen individuals from the two main islands of Guadeloupe, Grande Terre and Basse Terre. Taken together, these observations suggest that the morphological variability of past mimids was greater than at present, with traits or combinations of traits absent from current members of this family. In other words, the reduction or disappearance of island populations may have led to a reduction in intra-specific phenotypic variation, as has been argued, for example, for the morphological evolution of lizards in a similar Lesser Antillean context (Bochaton et al. 2017). Mimidae are currently represented in the West Indies in general and in the Lesser Antilles in particular, by several subspecies with marked differences in terms of population and range. Intra-specific genetic differences have also been demonstrated in studies of West Indian forest birds. The Scaly-breasted Thrasher appears to be structured in different genetically-related clusters between the different islands of the Lesser Antilles (Khimoun et al. 2016a) and within the islands of Guadeloupe between Basse Terre and Grande Terre. This has been interpreted to result from habitat fragmentation and the isolation of populations on each island over the past centuries (Khimoun et al. 2016b). It should therefore not be surprising that populations separated by several dozen kilometer wide inlets would have been sufficiently isolated to differentiate themselves to such a point that they display subtle osteological variations detectable by a geometric morphometric characterisation of their bones.

CONCLUSION

The different morphometric approaches revealed a robust correlation between phenotypic and phylogenic signals. Clear morphological differences separate the Antilleans endemics clade from the pan-continental clade, and inter-generic and inter-specific differences, respectively, were documented for the two clades, especially within the *Mimus* genus. These results complement previous molecular analyses. The GMM analysis equally isolates subtle morphological differences between these genera and species while conventional osteology helps describe diagnostic characters exhibited in modern specimens. A larger sample of Mimidae remains will likely increase the reliability of these characters. Combining GMM with conventional osteology equally provides a mean for reliably determining fossil specimens to species. The three taxa identified in the fossil sample were all recovered from the same island, Marie-Galante, and date from the Pleistocene to late Holocene. This includes the first mention of *Dumetella carolinensis* in the fossil record of the Lesser Antilles (*Abri Cadet 3)*, the presence of *Allenia fusca* at *Grotte Cadet 2* and *Cinclocerthia ruficauda* at *Grotte Blanchard*. The Brown Trembler was also found to have occurred over the last two millennia on La Désirade and the Eastern coast of Grande Terre, suggesting human activity to have directly or indirectly driven a contraction in their range.

DATA ACCESSIBILITY STATEMENT

Data are available in the supplementary files. 3D model from modern specimens are downloadable on MorphoSource (project MoMi) at: *https://www.morphosource.org/projects/000365016*

ADDITIONAL FILES

The additional files for this article can be found as follows:

- **Supplementary file 1.** Sample composition. Several specimens (in grey) were excluded from the initial sampling because they contained lead or were treated with products that interfered with the X-ray, leading to unusable scans. DOI: *https://doi.org/10.5334/oq.99.s1*
- **Supplementary file 2.** Geographical maps. A – Location of the Guadeloupe Islands within the Lesser Antilles. B – Ecological map of Guadeloupe Islands. The legend and ecological map are based on (Rousteau et al., 1994). The different fossil-bearing sites included in this study as white stars: 1 – Grotte des Bambous; 2 – Abri Cadet 3; 3 – Grotte Cadet 2; 4 – Grotte Blanchard; 5 – Pointe Gros Rempart 6. Isobaths (-200 m, from Münch et al. 2013) approximate the position of the coastline during the last marine lowstand. DOI: *https://doi.org/10.5334/oq.99.s2*
- **Supplementary file 3.** Position of the semi-landmarks (Zone 1 to 15 delineated circled in green) and landmarks (Lm 1 to Lm 5 circled in red). DOI: *https://doi.org/10.5334/oq.99.s3*
- **Supplementary file 4.** Complete dataset. DOI: *https://doi.org/10.5334/oq.99.s4*
- **Supplementary file 5.** Distal dataset. DOI: *https://doi.org/10.5334/oq.99.s5*

ACKNOWLEDGEMENTS

This study was conducted in the MoMi project funded by the LaScArBx ANR-10-LABX-52. It also benefited from funding and material collected in the ECSIT Project: « Écosystèmes insulaires tropicaux, réponse de la faune indigène terrestre de Guadeloupe à 6 000 ans d'anthropisation du milieu », with financial support from the European PO-FEDER program (grant n° 2016-FED-503), the Guadeloupe Regional Council, and the DAC of Guadeloupe.

The µCT equipment was acquired thanks to funding from Nouvelle-Aquitaine Regional Council & the Cluster of Excellence in Archaeological Sciences in Bordeaux (ANR-10-LABX-52).

The authors are grateful to the institutions and curators who facilitated the loans of comparative specimens: S. Guimaraes (MEC), J. Fuchs & C. Lefèvre (MNHN), M. Peck (ROM), J. White (NHM), P. Sweet (AMNH), C. Milensky (USNM). A special thanks to Janet Hinshaw and Matt Friedman of the UMMZ who very kindly made and shared the microscan of the *Ramphocinclus brachyurus* specimen housed in their institution.

The authors would also like to thank the Office National de la Chasse et de la Faune Sauvage de Guadeloupe (ONCFS), Anthony Levesque Birding enterprise and Luc Legendre of the DEAL Guadeloupe for facilitating the acquisition of mimidae specimens by the PACEA laboratory under the permits from the DEAL Guadeloupe for the possession and transport of specimens of protected species in 2011 (November 28th), 2013 (November 22nd), 2015 (30th April) and 2017 (February17th). We thank M. Boudadi-Maligne, who directed the 2011 PGR6 test-pit, for kindly granting us permission to include the material collected during this excavation as well as Pauline Hanot for her valuable methodological insight.

We would also like to thank Matthew Law for assistance during the reviewing process of this paper. We also acknowledge Markus Telkamp and an anonymous reviewer for their constructive comments on a first draft of the manuscript. Finally, we would like to thank Brad Gravina for the English editing of the manuscript.

COMPETING INTERESTS

The authors have no competing interests to declare.

AUTHOR CONTRIBUTIONS

MG, VL, RL and AL designed the project. NJ performed the analyses under the supervision of MG, AL, VL, RL and FS. All the authors interpreted the obtained data and wrote the manuscript. NJ prepared the figures, tables and supplementary information.

AUTHOR AFFILIATIONS

Nicolas Jeantet
PACEA UMR 5199, Université de Bordeaux, CNRS, MCC, France

Ronan Ledevin *orcid.org/0000-0002-1936-9612*
PACEA UMR 5199, Université de Bordeaux, CNRS, MCC, France

Monica Gala *orcid.org/0000-0002-4991-3332*
PACEA UMR 5199, Université de Bordeaux, CNRS, MCC, France

Arnaud Lenoble *orcid.org/0000-0001-9023-9741*
PACEA UMR 5199, Université de Bordeaux, CNRS, MCC, France

Frédéric Santos *orcid.org/0000-0003-1445-3871*
PACEA UMR 5199, Université de Bordeaux, CNRS, MCC, France

Véronique Laroulandie *orcid.org/0000-0002-9745-6578*
PACEA UMR 5199, Université de Bordeaux, CNRS, MCC, France

REFERENCES

Adams, D, Collyer, M, Kaliontzopoulou, A and **Baken, E.** 2021. Geometric morphometric analyses of 2D/3D landmark data. *2020*.

Adler, D, Murdoch, D, Nenadic, O, Urbanek, S, Chen, M, Gebhardt, A and **Senger, A.** 2019. rgl: 3D Visualization Using OpenGL. R package version 0.100. 19.

Aldridge, BM. 1984. Sympatry in two species of mockingbirds on Providenciales Island, West Indies. *The Wilson Bulletin*, 96(4): 603–618.

Arbogast, BS, Drovetski, SV, Curry, RL, Boag, PT, Seutin, G, Grant, PR, Grant, BR and **Anderson, DJ.** 2006. The origin and diversification of Galapagos mockingbirds. *Evolution*, 60(2): 370–382. DOI: *https://doi.org/10.1111/j.0014-3820.2006.tb01113.x*

Baumel, JJ and **Witmer, LM.** 1993. Osteologia. In Baumel, JJ, King, AS, Breazile, JE, Evans, HE and Vanden Berge, JC (eds.), *Handbook of avian anatomy: Nomina Anatomica Avium*, 23: 45–132. 2nd edition. Cambridge, MA: Publications of the Nuttall Ornithological Club.

Benito-Espinal, É and **Hautcastel, P.** 2003. *Les oiseaux des Antilles et leur nid*. PLB ed.

Birdlife. 2020. *https://www.birdlife.org/*.

Bochaton, C, Bailon, S, Herrel, A, Grouard, S, Ineich, I, Tresset, A and **Cornette, R.** 2017. Human impacts reduce morphological diversity in an insular species of lizard. *Proceedings of the Royal Society B: Biological Sciences*, 284(1857): 20170921. DOI: *https://doi.org/10.1098/rspb.2017.0921*

Bochaton, C, Grouard, S, Cornette, R, Ineich, I, Lenoble, A, Tresset, A and **Bailon, S.** 2015. Fossil and subfossil herpetofauna from Cadet 2 Cave (Marie-Galante, Guadeloupe Islands, FWI): evolution of an insular herpetofauna since the Late Pleistocene. *Comptes Rendus Palevol*, 14(2): 101–110. DOI: *https://doi.org/10.1016/j.crpv.2014.10.005*

Bond, J. 1948. Origin of the bird fauna of the West Indies. *The Wilson Bulletin*, 60(4): 207–229.

Bond, J. 1963. Derivation of the Antillean avifauna. *Proceedings of the Academy of Natural Sciences of Philadelphia*, 115(4): 79–98.

Bookstein, FL. 1997. Morphometric tools for landmark data: geometry and biology. first published 1991. Cambridge: Cambridge University Press. DOI: *https://doi.org/10.1017/CBO9780511573064*

Boudadi-Maligne, M, Bailon, S, Bochaton, C, Casagrande, F, Grouard, S, Serrand, N and **Lenoble, A.** 2016. Evidence for Historical Human-Induced Extinctions of Vertebrate Species on La Désirade (French West Indies). *Quaternary Research*, 85(1): 54–65. DOI: *https://doi.org/10.1016/j.yqres.2015.11.001*

Bovy, KM. 2002. Differential avian skeletal part distribution: explaining the abundance of wings. *Journal of archaeological Science*, 29(9): 965–978. DOI: *https://doi.org/10.1006/jasc.2001.0795*

Case, TJ, Faaborg, J and **Sidell, R.** 1983. The Role of Body Size in the Assembly of West Indies Bird Communities. *Evolution*, 37(5): 1062–1074. DOI: *https://doi.org/10.1111/j.1558-5646.1983.tb05633.x*

Cibois, A and **Cracraft, J.** 2004. Assessing the passerine "Tapestry": phylogenetic relationships of the Muscicapoidea inferred from nuclear DNA sequences. *Molecular phylogenetics and evolution*, 32(1): 264–273. DOI: *https://doi.org/10.1016/j.ympev.2003.12.002*

Cochard, D, Bochaton, C, Courtaud, P, Ephrem, B, Gala, M, Goedert, J, Lenoble, A, Partiot, C and **Royer, A.** 2019. *Grotte des Bambous, commune du Moule, Guadeloupe. Rapport d'opération de fouille archéologique*. Basse-Terre, Guadeloupe: DAC Guadeloupe, Service de l'Archéologie, 175.

Cody, ML. 2005. Mimidés. In del Hoyo, J, Elliot, A and Christie, D (eds.), *Cuckoo-shrikes to Thrushes*, 448–495. Handbook of the birds of the World, Vol 10. Barcelona: Lynx Edicions and Birdlife international.

Cooke, SB, Dávalos, LM, Mychajliw, AM, Turvey, ST and **Upham, NS.** 2017. Anthropogenic extinction dominates Holocene declines of West Indian mammals. *Annual Review of Ecology, Evolution, and Systematics*, 48: 301–327. DOI: *https://doi.org/10.1146/annurev-ecolsys-110316-022754*

Corbin, CE, Lowenberger, LK and **Dorkoski, RP.** 2013. The skeleton flight apparatus of North American bluebirds (Sialia): Phylogenetic thrushes or functional flycatchers? *Journal of morphology*, 274(8): 909–917. DOI: *https://doi.org/10.1002/jmor.20147*

Cucchi, T and **Evin, AMJ.** 2015. Morphométrie géométrique et archéozoologie: Concepts, méthodes et applications. In Balasse, M, Brugal, JP and Dauphin, Y (eds.), *Messages d'os Archéométrie du squelette animal et humain*, 197–216. Paris: Editions des archives contemporaines. DOI: *https://doi.org/10.17184/eac.3997*

Curtis, JH, Brenner, M and **Hodell, DA.** 2001. Climate change in the circum-Caribbean (Late Pleistocene to Present) and implications for regional biogeography. In Woods, CA and Sergile, FE (eds.), 35–54. Boca Raton: CRC Press. DOI: *https://doi.org/10.1201/9781420039481-3*

DaCosta, JM, Miller, MJ, Mortensen, JL, Reed, JM, Curry, RL and **Sorenson, MD.** 2019. Phylogenomics clarifies biogeographic and evolutionary history, and conservation status of West Indian tremblers and thrashers (Aves: Mimidae). *Molecular phylogenetics and evolution*, 136: 196–205. DOI: *https://doi.org/10.1016/j.ympev.2019.04.016*

Dray, S and **Dufour, AB.** 2007. The ade4 package: implementing the duality diagram for ecologists. *Journal of statistical software*, 22(4): 1–20. DOI: *https://doi.org/10.18637/jss.v022.i04*

eBird. 2021. eBird: An online database of bird distribution and abundance [web application]. eBird, Cornell Lab of Ornithology, Ithaca, New York. Available: *http://www.ebird.org*. (Accessed: Date [e.g., February 25, 2021]).

Gala, M and **Lenoble, A.** 2015. Evidence of the Former Existence of an Endemic Macaw in Guadeloupe, Lesser Antilles. *Journal of Ornithology*, 156(4): 1061–1066. DOI: *https://doi.org/10.1007/s10336-015-1221-6*

Hayes, FE and **Sewlal, JAN.** 2004. The Amazon River as a dispersal barrier to passerine birds: effects of river width, habitat and taxonomy. *Journal of Biogeography*, 31(11): 1809–1818. DOI: *https://doi.org/10.1111/j.1365-2699.2004.01139.x*

Hunt, JS, Bermingham, E and **Ricklefs, RE.** 2001. Molecular systematics and biogeography of Antillean thrashers, tremblers, and mockingbirds (Aves: Mimidae). *The Auk*, 118(1): 35–55. DOI: *https://doi.org/10.1093/auk/118.1.35*

Kessler, JE. 2015. Osteological guide of songbirds from Central Europe. *Ornis Hungarica*, 23(2): 62–155. DOI: *https://doi.org/10.1515/orhu-2015-0016*

Khimoun, A, Arnoux, E, Martel, G, Pot, A, Eraud, C, Condé, B, Loubon, M, Théron, F, Covas, R, Faivre, B and **Garnier, S.** 2016a. Contrasted patterns of genetic differentiation across eight bird species in the Lesser Antilles. *Genetica*, 144(1): 125–138. DOI: *https://doi.org/10.1007/s10709-016-9883-4*

Khimoun, A, Eraud, C, Ollivier, A, Arnoux, E, Rocheteau, V, Bely, M, Lefol, E, Delpuech, M, Carpentier, ML, Leblond, G, Levesque, A, Charbonnel, A, Faivre, B and **Garnier, S.** 2016b. Habitat specialization predicts genetic response to fragmentation in tropical birds. *Molecular ecology*, 25(16): 3831–3844. DOI: *https://doi.org/10.1111/mec.13733*

LeFebvre, MJ and **Sharpe, AE.** 2018. Contemporary challenges in zooarchaeological specimen identification. In Giovas, CM and LeFebvre, M (eds.), *Zooarchaeology in practice: Case Studies in Methodology and Interpretation in Archaeofaunal Analysis*, 35–57. Cham.: Springer. DOI: *https://doi.org/10.1007/978-3-319-64763-0_3*

Lenoble, A. 2014. Suivi archéologique des prélèvements pour analyse isotopique de la grotte Cadet 2. *Bilan scientifique Région Guadeloupe*, 2013: 147–148.

Lenoble, A, Gala, M and **Laroulandie, V.** 2019. The past and future of the University of Bordeaux's bird skeleton reference collection. *Alauda*, 87(3) (n° Hors-série-Actes du 10th International Meeting of European Curators, 17–19 oct. 2017, Paris): 83–92.

Lenoble, A, Stouvenot, C, Courtaud, P, Grouard, S, Scalliet, M and **Serrand, N.** 2009. Formes et remplissages du karst littoral guadeloupéen. In Vanara, N (ed.), *Le karst, indicateur performant des environnements passés. Karstologia*, n°17: 226–233. Mémoire.

Levesque, A and **Delcroix, F.** 2019. *Liste des oiseaux de la Guadeloupe (9ème édition). Grande-Terre, Basse-Terre, Marie-Galante, les Saintes, la Désirade, Îlets de la Petite Terre*. Rapport Amazona n°63. Les Abymes (Guadeloupe): Amazona. 23.

Levesque, A et **Delcroix, F.** 2021. Liste des oiseaux de l'île de la Désirade (2nde édition). Les Abymes (Guadeloupe): Amazona. 12.

Lovette, IJ, Arbogast, BS, Curry, RL, Zink, RM, Botero, CA, Sullivan, JP, Talaba AL, Harris RB, Rubenstein DR, Ricklefs RE and **Bermingham, E.** 2012. Phylogenetic relationships of the mockingbirds and thrashers (Aves: Mimidae). *Molecular Phylogenetics and Evolution*, 63(2): 219–229. DOI: *https://doi.org/10.1016/j.ympev.2011.07.009*

Lovette, IJ and **Rubenstein, DR.** 2007. A comprehensive molecular phylogeny of the starlings (Aves: Sturnidae) and mockingbirds (Aves: Mimidae): congruent mtDNA and nuclear trees for a cosmopolitan avian radiation. *Molecular phylogenetics and evolution*, 44(3): 1031–1056. DOI: *https://doi.org/10.1016/j.ympev.2007.03.017*

Mayr, G. 2016. *Avian evolution: the fossil record of birds and its paleobiological significance*. Chichester: John Wiley & Sons. (Series: Topics in paleobiology). DOI: *https://doi.org/10.1002/9781119020677*

Mitteroecker, P and **Gunz, P.** 2009. Advances in geometric morphometrics. *Evolutionary Biology*, 36(2): 235–247. DOI: *https://doi.org/10.1007/s11692-009-9055-x*

Moreno, E. 1985. Clave osteologica para la identificacion de los passeriformes ibericos. Sociedad Española de Ornitología. 1. Aegithalidae, Remizidae, Paridae, Emberizidae, Passeridae, Fringillidae, Alaudidae. *Ardeola*, 32(2): 295–377.

Moreno, E. 1986. Clave osteológica para la identificación de los Passeriformes ibéricos. 2. Hirundinidae, Prunellidae, Sittidae, Certhiidae, Troglodytidae, Cinclidae, Laniidae, Oriolidae, Corvidae, Sturnidae, Motacillidae. *Ardeola,* 33(1–2): 69–129.

Moreno, E. 1987. Clave osteológica para la identificación de los Passeriformes ibéricos. 3. Muscicapidae. *Ardeola*, 34(2): 243–273.

Mortensen, JL, Morton, MN, Haynes, P, Tschirky, J, Felix, ML and **Reed, JM.** 2017. Current status of the Endangered White-breasted Thrasher (*Ramphocinclus brachyurus*), a dry forest songbird endemic to Saint Lucia and Martinique. *Journal of Caribbean Ornithology*, 30(1): 39–48.

Mourer-Chauviré, C. 1975. Les oiseaux du Pléistocène moyen et superieur de France. Documents des laboratoires de la Faculté des Sciences de Lyon, n°64: 624.

Olson, SL. 1978. A paleontological perspective of West Indian birds and mammals. In Gill, FB (ed.) *Zoogeography of the Caribbean, The 1975 Leidy Medal Symposium*, 13: 99–117. Academy of Natural Sciences of Philadelphia, Special Publication.

Olson, SL and **Hilgartner, WB.** 1982. Fossil and Subfossil Birds of the Bahamas. In Olson, SL (ed.), *Fossil Vertebrates from the Bahamas*, 22–56. (Smithsonian Contributions to Paleobiology 48). Washington: Smithsonian Institution Press. DOI: *https://doi.org/10.5479/si.00810266.48.1*

Orihuela, J, Viñola, LW, Vázquez, OJ, Mychajliw, AM, Hernández de Lara, OH, Lorenzo, L and **Soto-Centeno, JA.** 2020. Assessing the role of humans in Greater Antillean land vertebrate extinctions: New insights from Cuba. *Quaternary Science Reviews*, 249: 106597. DOI: *https://doi.org/10.1016/j.quascirev.2020.106597*

Pregill, GK, Steadman, DW, Olson, SL and **Grady, FV.** 1988. *Late Holocene fossil vertebrates from Burma Quarry, Antigua, Lesser Antilles*. (Smithsonian contributions to Zoology 463). Washington: Smithsonian Institution Press. 27p. DOI: *https://doi.org/10.5479/si.00810282.463*

Pregill, GK, Steadman, DW and **Watters, DR.** 1994. Late Quaternary vertebrate faunas of the Lesser Antilles: historical components of Caribbean biogeography. *Bulletin of Carnegie Museum of Natural History*, 30: 1–51.

R Core Team. 2019. *R: A language and environment for statistical computing*. Vienna, Austria: R Foundation for Statistical Computing. URL *https://www.R-project.org/*.

Raffaele, HA. 2003. *Birds of the West Indies*. Princeton: Princeton University Press, Princeton field guides. 216.

Raffaele, HA, Wiley, J, Garrido, OH, Keith, A and **Raffaele, JI.** 2010. *Birds of the West indies*. Princeton: Princeton University Press.

Ricklefs, R and **Bermingham, E.** 2008. The West Indies as a laboratory of biogeography and evolution. *Philosophical Transactions of the Royal Society B: Biological Sciences*, 363(1502): 2393–2413. DOI: *https://doi.org/10.1098/rstb.2007.2068*

Royer, A, Malaizé, B, Lécuyer, C, Queffelec, A, Charlier, K, Caley, T and **Lenoble, A.** 2017. A high-resolution temporal record of environmental changes in the Eastern Caribbean (Guadeloupe) from 40 to 10 ka BP. *Quaternary Science Reviews*, 155: 198–212. DOI: *https://doi.org/10.1016/j.quascirev.2016.11.010*

Schlager, S. 2017. Morpho and Rvcg-Shape Analysis in R. In Zheng, G, Li, S and Szekely, G (eds.), *Statistical Shape and Deformation Analysis*. Academic Press. DOI: *https://doi.org/10.1016/B978-0-12-810493-4.00011-0*

Steadman, DW, Norton, RL, Browning, RM and **Arendt, W.** 1997. Birds of St. Kitts. *Caribbean Journal of Science,* 33(1–2): 1–20.

Steadman, DW, Pregill, GK and **Olson, SL.** 1984. Fossil vertebrates from Antigua, Lesser Antilles: evidence for late Holocene human-caused extinctions in the West Indies. *Proceedings of the National Academy of Sciences*, 81(14): 4448–4451. DOI: *https://doi.org/10.1073/pnas.81.14.4448*

Steadman, DW and **Franklin, J.** 2017. Origin, paleoecology, and extirpation of bluebirds and crossbills in the Bahamas across the last glacial–interglacial transition. *Proceedings of the National Academy of Sciences*, 114(37): 9924–9929. DOI: *https://doi.org/10.1073/pnas.1707660114*

Steadman, DW and **Franklin, J.** 2020. Bird populations and species lost to Late Quaternary environmental change and human impact in the Bahamas. *Proceedings of the National Academy of Sciences*, 117(43): 26833–26841. DOI: *https://doi.org/10.1073/pnas.2013368117*

Steadman, DW and **Takano, OM.** 2013. A late-Holocene bird community from Hispaniola: refining the chronology of vertebrate extinction in the West Indies. *The Holocene*, 23(7): 936–944. DOI: *https://doi.org/10.1177/0959683613479683*

Stewart, JR. 2005. The use of modern geographical ranges in the identification of archaeological bird remains. In Grupe, G and Peters, J (eds.), *Feathers, Grit and Symbolism: Birds and Humans in the Ancient Old and New Worlds*, 3: 43–54. Proceedings of the 5th Meeting of the ICAZ Bird Working Group in Munich. Documenta Archaeobiologiae.

Stewart, JR. 2007. *The Evolutionary Study of Some Archaeologically Significant Avian Taxa in the Quaternary of the Western Palaearctic*. BAR International Series 1653. Oxford: Archaeopress. DOI: *https://doi.org/10.30861/9781407300894*

Stoetzel, E, Royer, A, Cochard, D and **Lenoble, A.** 2016. Late Quaternary changes in bat palaeobiodiversity and palaeobiogeography under climatic and anthropogenic pressure: new insights from Marie-Galante, Lesser Antilles. *Quaternary Science Reviews*, 143: 150–174. DOI: *https://doi.org/10.1016/j.quascirev.2016.05.013*

Storer, RW. 1989. Geographic variation and sexual dimorphism in the tremblers (*Cinclocerthia*) and White-breasted Thrasher (*Ramphocinclus*). *The Auk*, 106(2): 249–258.

Stouvenot, C, Grouard, S, Bailon, S, Bonnissent, D, Lenoble, A, Serrand, N and **Sierpe, V.** 2014. L'abri sous roche Cadet 3 (Marie-Galante): un gisement à accumulations de faune et à vestiges archéologiques. In Bérard, B (ed.), *Actes du 24e Congrès de l'AIAC*, 126–140. Fort-de-France, Martinique.

Tellkamp, MP. 2005. *Prehistoric exploitation and biogeography of birds in coastal and Andean Ecuador*. Unpublished thesis (PhD), University of Florida.

Terborgh, J, Faaborg, J and **Brockmann, HJ.** 1978. Island colonization by Lesser Antillean birds. *The Auk*, 95(1): 59–72. DOI: *https://doi.org/10.2307/4085495*

Tomek, T and **Bocheński, ZM.** 2000. *The comparative osteology of European corvids (Aves: Corvidae), with a key to the identification of their skeletal elements*. Krakow: Instytutu Systematyki i Ewolucji Zwierząt PAN.

Von den Driesch, A. 1976. *A guide to the measurement of animal bones from archaeological sites: as developed by the Institut für Palaeoanatomie, Domestikationsforschung und Geschichte der Tiermedizin of the University of Munich* (Vol. 1). Peabody Museum Press.

Weber, GW and **Bookstein, FL.** 2011. *Virtual anthropology: a guide to a new interdisciplinary field*. Springer Verlag. DOI: *https://doi.org/10.1007/978-3-211-49347-2*

Wetmore, A. 1943. The birds of southern Veracruz, Mexico. *Proc. US Natl. Mus*. 93: 215–340. DOI: *https://doi.org/10.5479/si.00963801.93-3164.215*

Wils, P. 2016. Post-traitement des données du CTscan avec Avizo Lite 9.0.1. *http://www.ums2700.mnhn.fr/ast-rx/ressources*.

Wojcik, JD. 2002. The comparative osteology of the humerus in European thrushes (Aves: *Turdus*) including a comparison with other similarly sized genera of passerine birds-preliminary results. *Acta zoologica cracoviensia*, 45: 369–381.

Zusi, RL. 1969. Ecology and adaptations of the Trembler on the island of Dominica. *Living Bird*, 8: 137–164.

TO CITE THIS ARTICLE:
Jeantet, N, Ledevin, R, Gala, M, Lenoble, A, Santos, F and Laroulandie, V. 2021. Investigating Past and Present Carpometacarpus Morphology in Mimidae: A Multi-Methods Approach to Evidence from the Guadeloupe Islands. *Open Quaternary*, 7: 10, pp. 1–27. DOI: *https://doi.org/10.5334/oq.99*

Submitted: 07 April 2021 Accepted: 14 October 2021 Published: 22 December 2021